Electronic Supplementary Material (ESI) for RSC Advances.


*Supplementary Materials*

# Multifunctional Biphenyl Derivatives As Photosensitizers In Various Types Of Photopolymerization Processes, Including IPNs Formation, 3D Printing And The Manufacture Of Photo-Curable CNTs Composites

Wiktoria Tomal[1], Anna Chachaj-Brekiesz[3], Roman Popielarz[1], Joanna Ortyl*[1,2]

[1] Cracow University of Technology, Faculty of Chemical Engineering and Technology, Warszawska 24, 31-155 Cracow, Poland

[2] Photo HiTech Ltd., Bobrzyńskiego 14, 30-348 Cracow, Poland

[3] Jagiellonian University, Faculty of Chemistry, Gronostajowa 2, 30-387 Cracow, Poland

* Correspondance: jortyl@pk.edu.pl

## Synthesis of 2-(diethylamino)-4-(1-ethylpropyl)-6-phenyl-benzene-1,3-dicarbonitrile derivatives

### Materials and methods

2-amino-4-methyl-6-arylbenzene-1,3-dicarbonitrile derivatives used for synthesis of target compounds were obtained following recently published procedure[1]. *N*,*N*-dimethylformamide was dried over freshly activated 4Å molecular sieves. Other reagents for synthesis were supplied from commercial sources and used without any further purification.

Structure and purity of synthesised compounds was confirmed with nuclear magnetic resonance spectra, mass spectrometry and liquid chromatography. $^{1}H$ and $^{13}C$ NMR spectra were recorded in DMSO-$D_6$ on Advance III HD 400 MHz (Bruker) spectrometer. Chemical shifts were reported in parts per million (δ) and referenced to residual protonated solvent peak (δ = 2.50 ppm in $^{1}$HNMR or δ = 39.52 ppm in $^{13}$CNMR). LC-MS analyses were obtained on LCMS-2020 (Shimadzu) with ESI ionization method.

### General synthetic procedure for 2-(diethylamino)-4-(1-etylpropyl)-6-phenylbenzene-1,3-dicarbonitrile derivatives

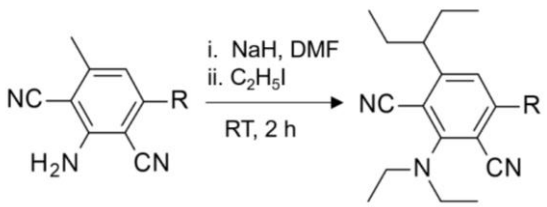


R = phenyl (BI-PH), phenyl-$CH_3$ (BI-PH-$CH_3$), phenyl-O-$CH_3$ (BI-PH-O-$CH_3$), phenyl-CN (BI-PH-CN), phenyl-$SO_2CH_3$ (BI-PH-$SO_2CH_3$), phenyl-S-$CH_3$ (BI-PH-S-$CH_3$), phenyl-$CF_3$ (BI-PH-$CF_3$), 1-naphtyl (BI-1-NPH), 2-naphtyl (BI-2-NPH), 9-anthyl (BI-9-AN)

The solution of appropriate 2-amino-4-methyl-6-arylbenzene-1,3-dicarbonitrile derivative (0.50 mmol) in *N*,*N*-dimethylformamide (2.0 mL) was added dropwise to the suspension of 60% sodium hydride (4.00 mmol, 160 mg) in *N*,*N*-dimethylformamide (2.0 mL). The resulting brownish suspension was stirred under nitrogen for 20 minutes. Then iodoethane (312 mg, 2.00 mmol) was added and stirring was continued. When thin layer chromatography showed no traces of 2-amino-4-methyl-6-arylbenzene-1,3-dicarbonitrile (usually after 1 h 40 min) water (10 mL) was added. The product was isolated by extraction with chloroform and purified by column chromatography on silica gel using chloroform as eluent.

**Physicochemical data for synthesized 2-(diethylamino)-4-(1-ethylpropyl)-6-phenylbenzene-1,3-dicarbonitrile derivatives**

| | |
|---|---|
| **BI-PH**<br> 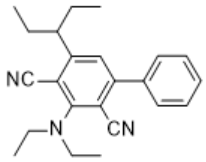 <br>*2-(diethylamino)-4-(1-ethylpropyl)-6-phenylbenzene-1,3-dicarbonitrile* | Obtained from 2-amino-4-methyl-6-phenylbenzene-1,3-dicarbonitrile (117 mg) in 140 mg (81%) yield.<br><br>Purity (LC): 96%<br><br>$^{1}$H NMR (400 MHz, DMSO) δ 7.64 – 7.60 (m, 2H), 7.56 – 7.51 (m, 3H), 7.30 (s, 1H), 3.48 (q, J = 7.1 Hz, 4H), 2.94 – 2.83 (m, 1H), 1.83 – 1.61 (m, 4H), 1.08 (t, J = 7.1 Hz, 6H), 0.77 (t, J = 7.4 Hz, 6 H).<br><br>$^{13}$C NMR (101 MHz, DMSO) δ 157.78, 155.79, 150.27, 137.09, 129.42, 129.00, 128.63, 123.10, 116.64, 116.13, 111.97, 108.81, 47.38, 46.88, 27.86, 13.47, 11.84.<br><br>MS (ESI), m/z (%): 346 (100%, $[M+H]^+$) |
| **BI-PH-CH$_3$**<br> 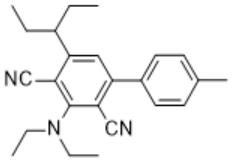 <br>*2-(diethylamino)-4-(1-ethylpropyl)-6-(4-methylphenyl)benzene-1,3-dicarbonitrile* | Obtained from 2-amino-4-(4-methylphenyl)-6-methyl-benzene-1,3-dicarbonitrile (124 mg) in 100 mg (56%) yield.<br><br>Purity (LC): 99%<br><br>$^{1}$H NMR (400 MHz, DMSO) δ 7.55 – 7.50 (m, 2H), 7.38 – 7.32 (m, 2H), 7.27 (s, 1H), 3.47 (q, J = 7.1 Hz, 4H), 2.92 – 2.83 (m, 1H), 2.39 (s, 3H), 1.84-1.58 (m, 4H), 1.08 (t, J = 7.1 Hz, 6H), 0.78 (t, J = 7.4 Hz, 6H).<br><br>$^{13}$C NMR (101 MHz, DMSO) δ 157.82, 155.69, 150.28, 139.21, 134.20, 129.22, 128.92, 122.96, 116.76, 116.19, 111.70, 108.70, 47.35, 46.88, 27.88, 20.81, 13.48, 11.85.<br><br>MS (ESI), m/z (%): 360 (100%, $[M+H]^+$) |
| **BI-PH-O-CH$_3$**<br> 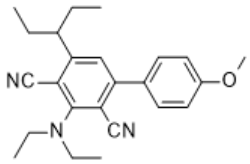 <br>*2-(diethylamino)-6-(1-ethylpropyl)-4-(4-methoxyphenyl) benzene-1,3-dicarbonitrile* | Obtained from 2-amino-4-(4-methoxyphenyl)-6-methyl-benzene-1,3-dicarbonitrile (132 mg) in 80 mg (43%) yield.<br><br>Purity (LC): 87%<br><br>$^{1}$H NMR (400 MHz, DMSO) δ 7.62 – 7.55 (m, 2H), 7.26 (s, 1H), 7.12 – 7.06 (m, 2H), 3.83 (s, 3H), 3.47 (q, J = 7.1 Hz, 4H), 2.92 – 2.81 (m, 1H), 1.84 -1.61 (m, 4H), 1.07 (t, J = 7.1 Hz, 6H), 0.78 (t, J = 7.4 Hz, 6H).<br><br>$^{13}$C NMR (101 MHz, DMSO) δ 160.32, 157.88, 155.57, 149.99, 130.52, 129.19, 122.83, 116.90, 116.24, 114.10, 111.33, 108.57, 55.36, 47.33, 46.87, 27.88, 13.48, 11.85.<br><br>MS (ESI), m/z (%): 376 (100%, $[M+H]^+$) |
| **BI-PH-CN**<br> 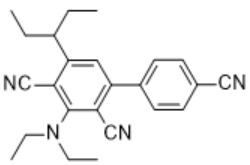 <br>*4-(4-cyanophenyl)-2-(diethylamino)-6-(1-ethylpropyl)benzene-1,3-dicarbonitrile* | Obtained from 2-amino-4-(4-cyanophenyl)-6-methyl-benzene-1,3-dicarbonitrile (129 mg) in 110 mg (59%) yield.<br><br>Purity (LC): 99%<br><br>$^{1}$H NMR (400 MHz, DMSO) δ 8.06 – 7.99 (m, 2H), 7.89 – 7.82 (m, 2H), 7.36 (s, 1H), 3.49 (q, J = 7.1 Hz, 4H), 2.94 – 2.84 (m, 1H), 1.85 – 1.61 (m, 4H), 1.09 (t, J = 7.1 Hz, 6H), 0.78 (t, J = 7.4 Hz, 6H).<br><br>$^{13}$C NMR (101 MHz, DMSO) δ 157.77, 156.19, 148.45, 141.59, 132.47, 130.18, 122.98, 118.39, 116.37, 116.00, 112.57, 112.09, 108.59, 47.48, 46.81, 27.84, 13.45, 11.85.<br><br>MS (ESI), m/z (%): 371 (100%, $[M+H]^+$) |
| **BI-PH-SO$_2$-CH$_3$** | Obtained from 2-amino-4-methyl-6-(4-methylsulfonylphenyl)benzene-1,3- |

| | |
|---|---|
| 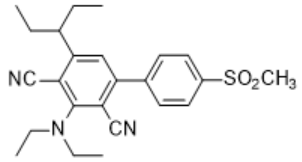 <br>*2-(diethylamino)-4-(1-ethylpropyl)-6-(4-methylsulfonylphenyl)benzene-1,3-dicarbonitrile* | dicarbonitrile (156 mg) in 154 mg (73%) yield.<br><br>Purity (LC): 86%<br><br>$^{1}$H NMR (400 MHz, DMSO) δ 8.12 – 8.06 (m, 2H), 7.94 – 7.88 (m, 2H), 7.37 (s, 1H), 3.50 (q, J = 7.1 Hz, 4H), 3.33 (s, 3H), 2.95 – 2.84 (m, 1H), 1.87 - 1.62 (m, 4H), 1.09 (t, J = 7.1 Hz, 6H), 0.78 (t, J = 7.4 Hz, 6H).<br><br>$^{13}$C NMR (101 MHz, DMSO) δ 157.79, 156.17, 148.53, 141.94, 141.49, 130.17, 127.15, 123.15, 116.40, 116.01, 112.59, 108.64, 47.47, 46.83, 43.29, 27.85, 13.47, 11.87.<br><br>MS (ESI), m/z (%): 424 (100%, $[M+H]^+$) |
| **BI-PH-S-CH$_3$**<br> 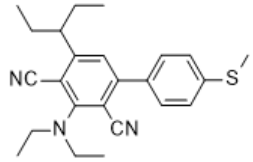 <br>*2-(diethylamino)-4-(1-ethylpropyl)-6-(4-methylsulfanylphenyl)benzene-1,3-dicarbonitrile* | Obtained from 2-amino-4-methyl-6-(4-methylsulfanylphenyl)benzene-1,3-dicarbonitrile (143 mg) in 100 mg (51%) yield.<br><br>Purity (LC): 99%<br><br>$^{1}$H NMR (400 MHz, DMSO) δ 7.60 – 7.55 (m, 2H), 7.42 – 7.37 (m, 2H), 7.28 (s, 1H), 3.47 (q, J = 7.0 Hz, 4H), 2.93 – 2.83 (m, 1H), 2.54 (s, 3H), 1.84 - 1.60 (m, 4H), 1.08 (t, J = 7.1 Hz, 6H), 0.78 (t, J = 7.4 Hz, 6H).<br><br>$^{13}$C NMR (101 MHz, DMSO) δ 157.89, 155.76, 149.72, 140.55, 133.18, 129.49, 125.49, 122.83, 116.76, 116.19, 111.65, 108.52, 47.36, 46.86, 27.87, 14.28, 13.48, 11.85.<br><br>MS (ESI), m/z (%): 392 (100%, $[M+H]^+$) |
| **BI-PH-CF$_3$**<br> 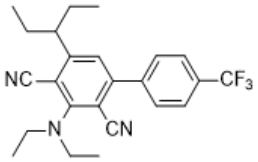 <br>*2-(diethylamino)-4-(1-ethylpropyl)-6-[4-(trifluoromethyl)phenyl]benzene-1,3-dicarbonitrile* | Obtained from 2-amino-4-methyl-6-[4-(trifluoromethyl)phenyl]benzene-1,3-dicarbonitrile (151 mg) in 60 mg (29%) yield.<br><br>Purity (LC): 95%<br><br>$^{1}$H NMR (400 MHz, DMSO) δ 7.94 – 7.89 (m, 2H), 7.89 – 7.84 (m, 2H), 7.37 (s, 1H), 3.49 (q, J = 7.1 Hz, 4H), 2.95 – 2.85 (m, 1H), 1.85 – 1.62 (m, 4H), 1.09 (t, J = 7.1 Hz, 6H), 0.78 (t, J = 7.4 Hz, 6H).<br><br>$^{13}$C NMR (101 MHz, DMSO) δ 157.74, 156.15, 148.72, 141.14 (q, J = 1.3 Hz), 130.08, 129.62 (q, J = 32.0 Hz), 125.47 (q, J = 3.6 Hz), 123.12, 125.05 (q, J = 272.5 Hz), 116.42, 116.02, 112.53, 108.72, 47.46, 46.84, 27.85, 13.46, 11.85.<br><br>MS (ESI), m/z (%): 414 (100%, $[M+H]^+$) |
| **BI-1-NPH**<br> 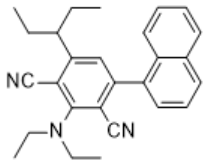 <br>*2-(diethylamino)-4-(1-ethylpropyl)-6-(1-naphthyl)benzene-1,3-dicarbonitrile* | Obtained from 2-amino-4-methyl-6-(1-naphthyl)benzene-1,3-dicarbonitrile (142 mg) in 160 mg (81%) yield.<br><br>Purity (LC): 92%<br><br>$^{1}$H NMR (400 MHz, DMSO) δ 8.11 – 8.04 (m, 2H), 7.67 – 7.52 (m, 4H), 7.43 – 7.39 (m, 1H), 7.34 (s, 1H), 3.48 (q, J = 7.1 Hz, 4H), 3.00 – 2.90 (m, 1H), 1.84 – 1.57 (m, 4H), 1.11 (t, J = 7.1 Hz, 6H), 0.87 – 0.75 (m, 6H).<br><br>$^{13}$C NMR (101 MHz, DMSO) δ 157.21, 155.64, 149.27, 135.02, 133.12, 130.49, 129.40, 128.58, 127.35, 127.19, 126.35, 125.33, 124.68, 124.26, 116.11, 115.98, 112.65, 110.71, 47.29, 46.92, 27.91, 27.68, 13.45, 11.85, 11.76.<br><br>MS (ESI), m/z (%): 396 (100%, $[M+H]^+$) |
| **BI-2-NPH** | Obtained from 2-amino-4-methyl-6-(2-naphthyl)benzene-1,3-dicarbonitrile (142 |

| | |
|---|---|
| 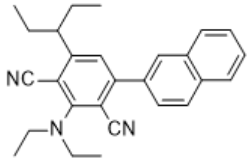 <br>*2-(diethylamino)-4-(1-ethylpropyl)-6-(2-naphthyl)benzene-1,3-dicarbonitrile* | mg) in 129 mg (65%) yield.<br><br>Purity (LC): 97%<br><br>$^{1}$H NMR (400 MHz, DMSO) δ 8.21 (s, 1H), 8.11 – 8.00 (m, 3H), 7.74 (dd, J = 8.5, 1.9 Hz, 1H), 7.66 – 7.60 (m, 2H), 7.44 (s, 1H), 3.51 (q, J = 7.1 Hz, 4H), 2.97 – 2.86 (m, 1H), 1.88 – 1.64 (m, 4H), 1.11 (t, J = 7.1 Hz, 6H), 0.81 (t, J = 7.4 Hz, 6H).<br><br>$^{13}$C NMR (101 MHz, DMSO) δ 157.80, 155.87, 150.33, 134.53, 132.93, 132.53, 128.59, 128.44, 128.17, 127.61, 127.26, 126.81, 126.42, 123.36, 116.75, 116.19, 111.98, 109.01, 47.46, 46.93, 27.93, 13.50, 11.90.<br><br>MS (ESI), m/z (%): 396 (100%, $[M+H]^+$) |
| **BI-1-AN**<br> 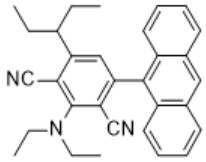 <br>*4-(9-anthryl)-2-(diethylamino)-6-(1-ethylpropyl)benzene-1,3-dicarbonitrile* | Obtained from 2-amino-4-(9-anthryl)-6-methylbenzene-1,3-dicarbonitrile (167 mg) in 40 mg (18%) yield.<br><br>Purity (LC): 72%<br><br>$^{1}$H NMR (400 MHz, DMSO) δ 8.82 (s, 1H), 8.28 – 8.19 (m, 2H), 7.62 – 7.50 (m, 4H), 7.42 (s, 1H), 7.38 – 7.33 (m, 2H), 3.49 (q, J = 7.1 Hz, 4H), 3.08 - 2.97 (m, 1H), 1.82 – 1.58 (m, 4H), 1.13 (t, J = 7.1 Hz, 6H), 0.83 (t, J = 7.4 Hz, 6H).<br><br>$^{13}$C NMR (101 MHz, DMSO) δ 157.28, 156.11, 147.94, 134.57, 131.09, 130.71, 129.04, 128.81, 128.41, 127.15, 125.57, 124.43, 116.10, 115.66, 113.30, 111.78, 47.28, 47.00, 27.74, 13.43, 11.75.<br><br>MS (ESI), m/z (%): 446 (100%, $[M+H]^+$) |

## NMR spectra for 2-(diethylamino)-4-(1-ethylpropyl)-6-phenylbenzene-1,3-dicarbonitrile derivatives

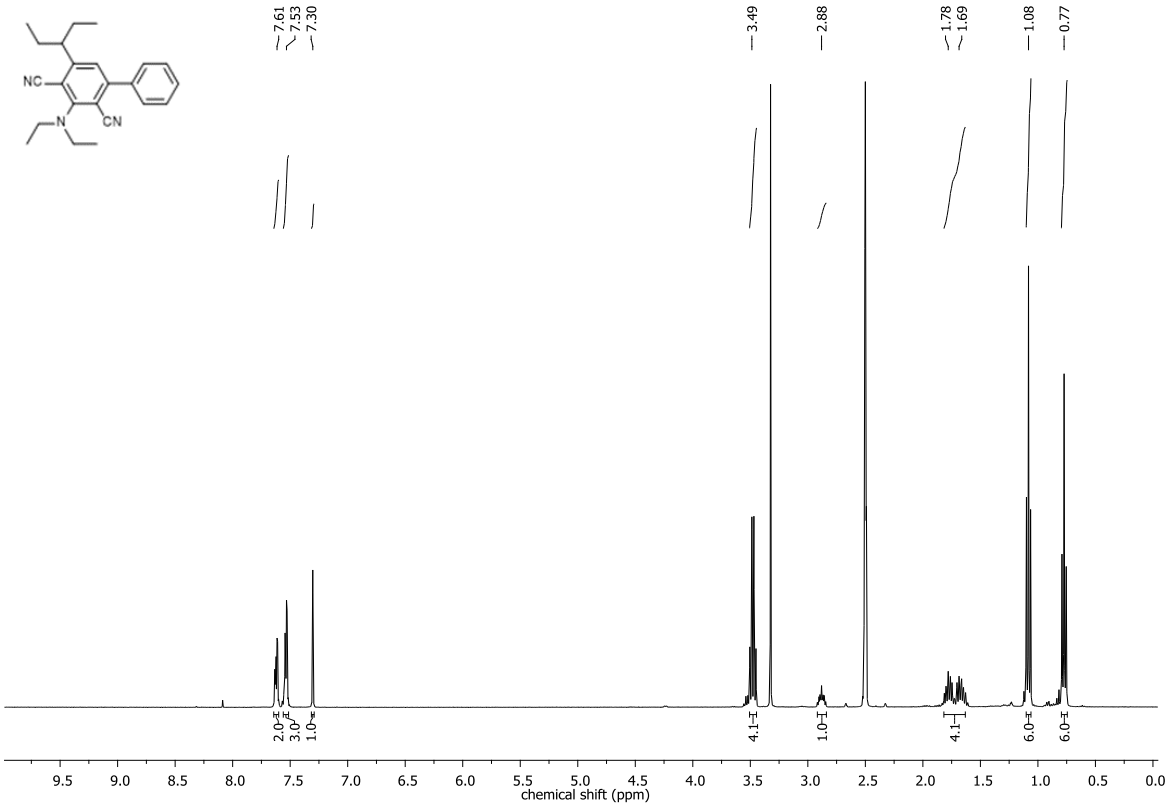


**Figure S1.** $^{1}$HNMR of 2-(diethylamino)-4-(1-ethylpropyl)-6-phenylbenzene-1,3-dicarbonitrile (**BI-PH**).

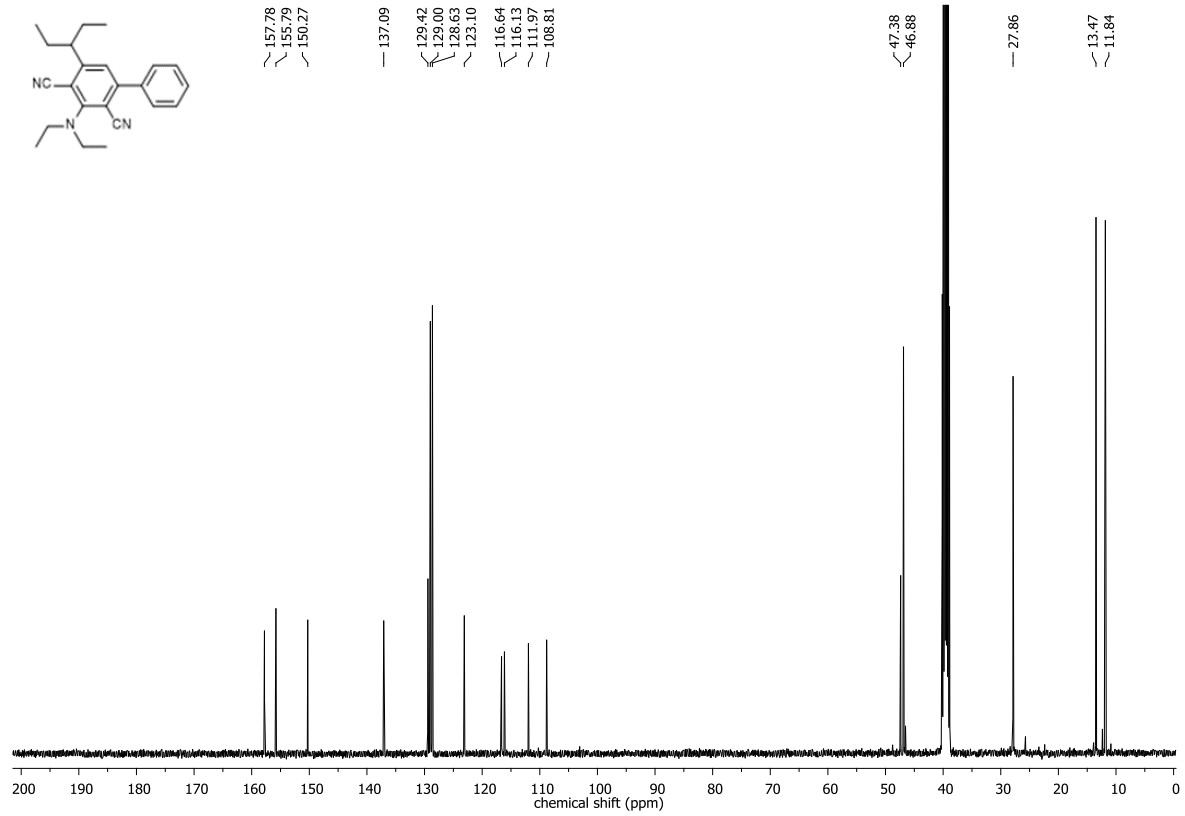


**Figure S2.** $^{13}$CNMR of 2-(diethylamino)-4-(1-ethylpropyl)-6-phenylbenzene-1,3-dicarbonitrile (**BI-PH**).

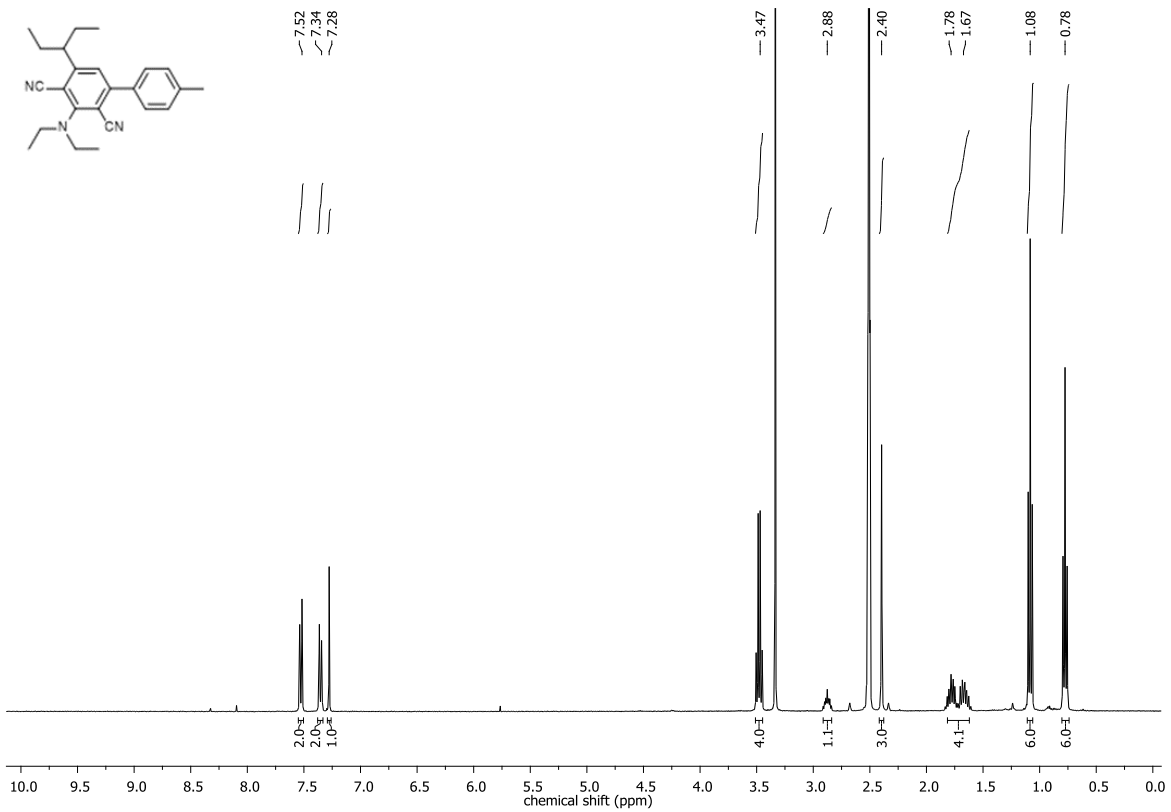


**Figure S3.** $^{1}$HNMR of 2-(diethylamino)-4-(1-ethylpropyl)- 6-(4-methylphenyl)benzene-1,3-dicarbonitrile (**BI-PH-CH$_3$**).

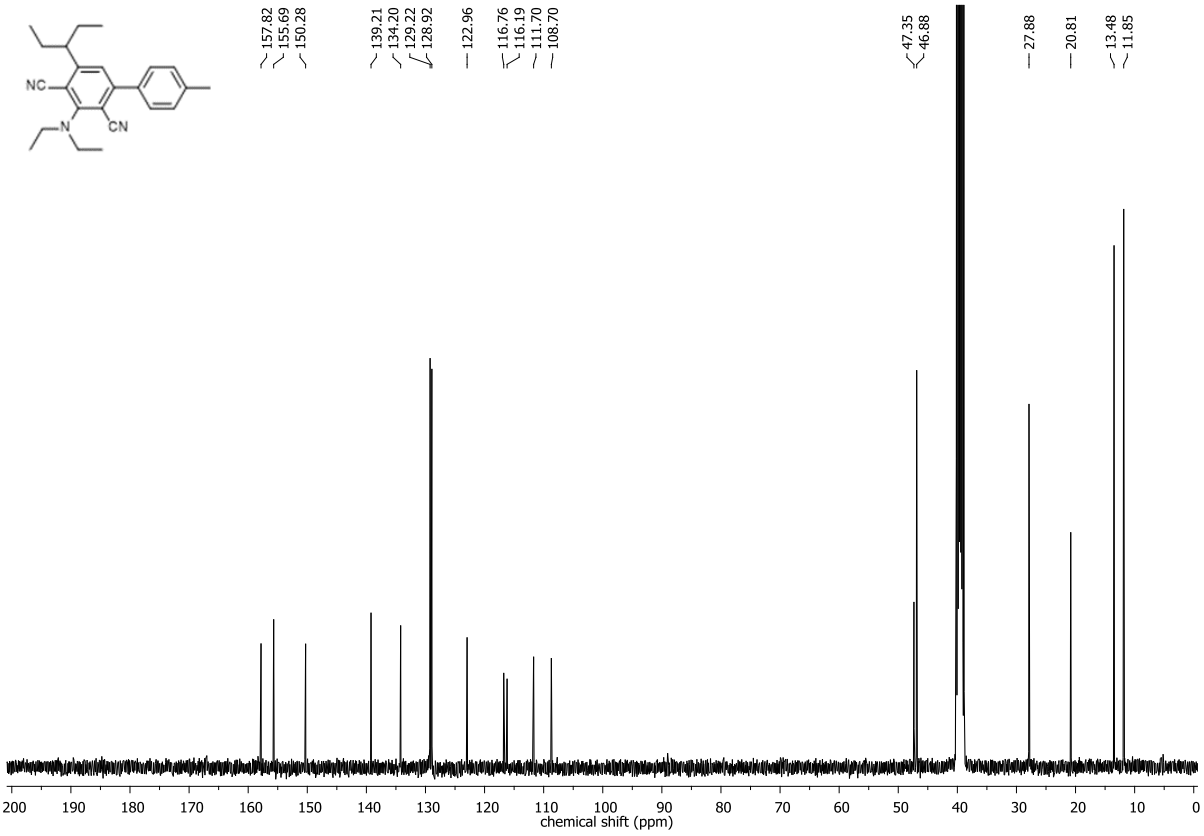


**Figure S4.** $^{13}$CNMR of 2-(diethylamino)-4-(1-ethylpropyl)- 6-(4-methylphenyl)benzene-1,3-dicarbonitrile (**BI-PH-CH$_3$**).

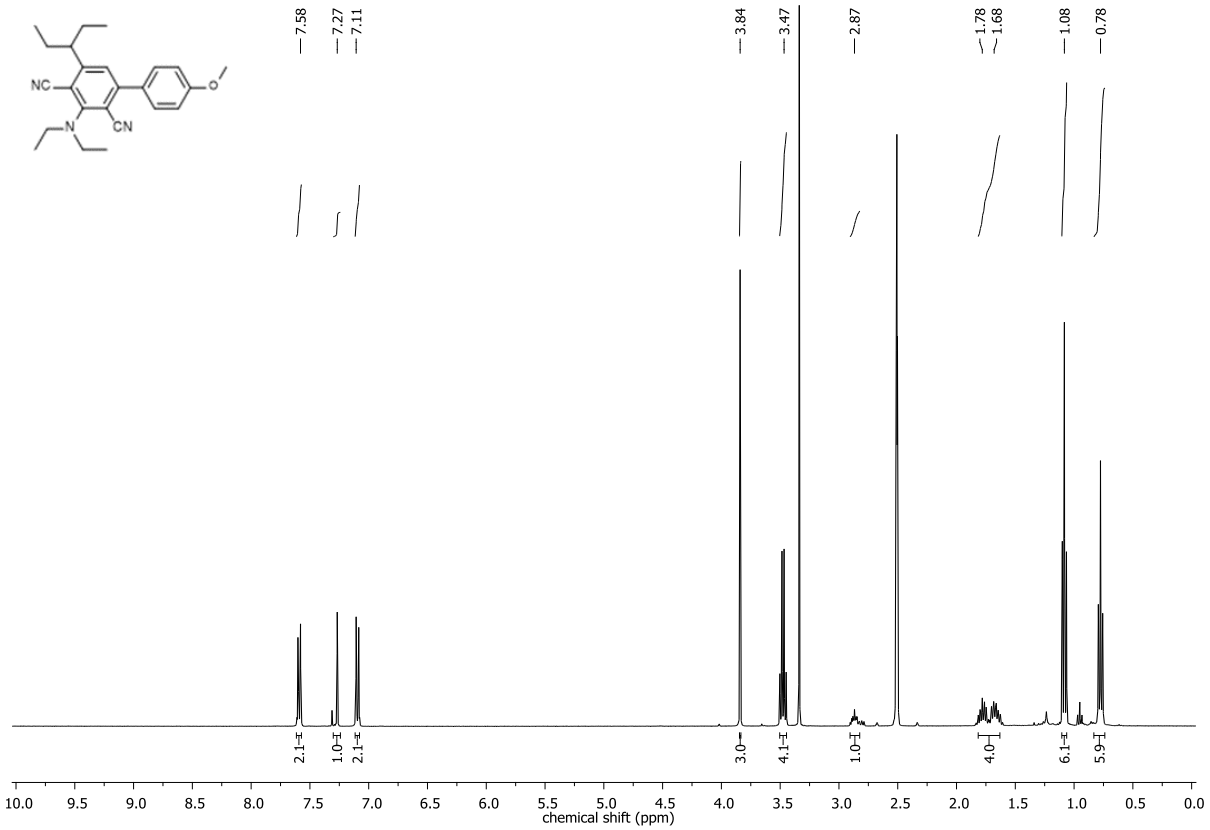


**Figure S5.** [1]HNMR of 2-(diethylamino)-6-(1-ethylpropyl)-4-(4-methoxyphenyl) benzene-1,3-dicarbonitrile (**BI-PH-O-$CH_3$**).

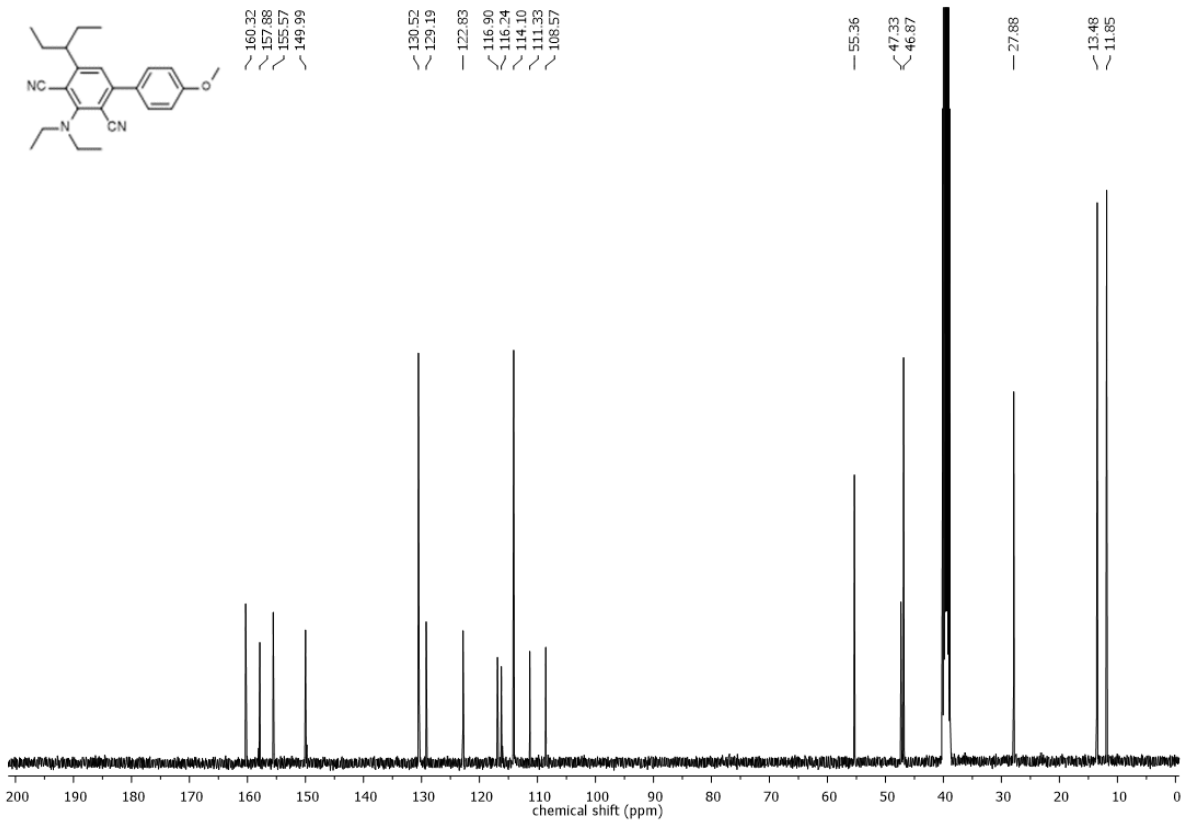


**Figure S6.** [13]CNMR of 2-(diethylamino)-6-(1-ethylpropyl)-4-(4-methoxyphenyl) benzene-1,3-dicarbonitrile (**BI-PH-O-$CH_3$**).

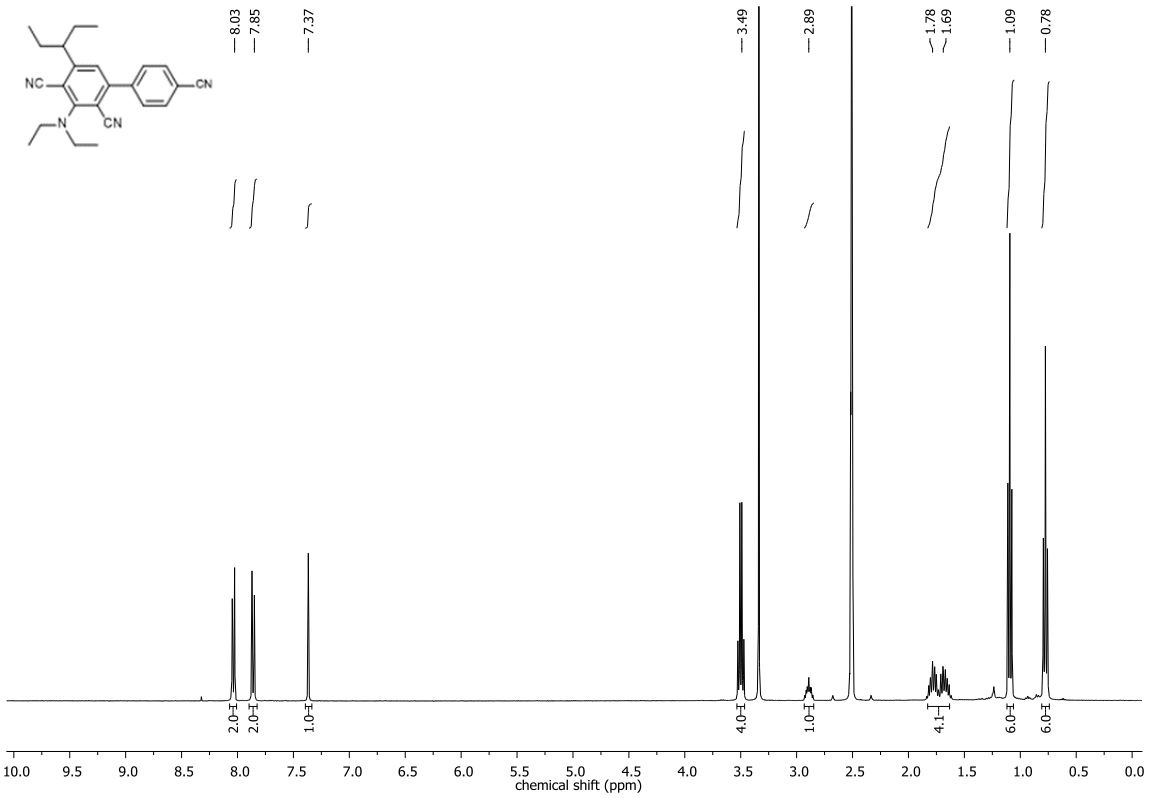


**Figure S7.** [1]HNMR of 4-(4-cyanophenyl)-2-(diethylamino)-6-(1-ethylpropyl)benzene-1,3-dicarbonitrile (**BI-PH-CN**).

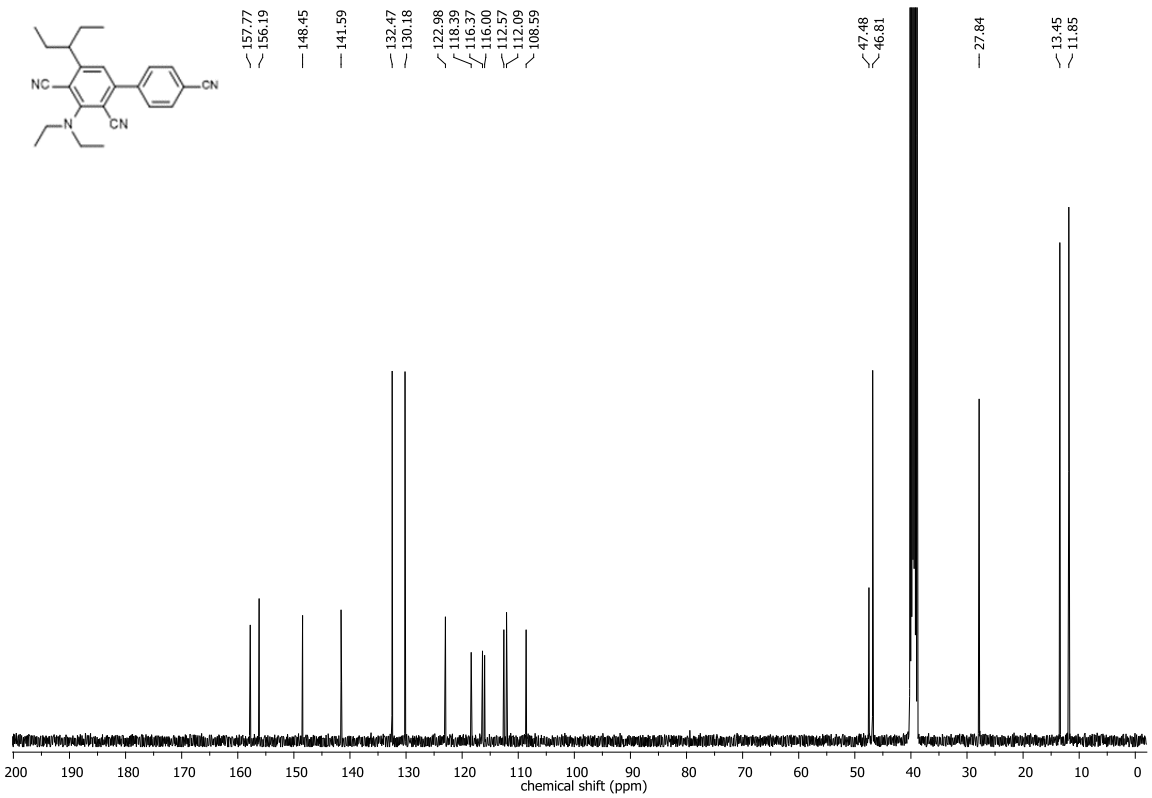


**Figure S8.** [13]CNMR of 4-(4-cyanophenyl)-2-(diethylamino)-6-(1-ethylpropyl)benzene-1,3-dicarbonitrile (**BI-PH-CN**).

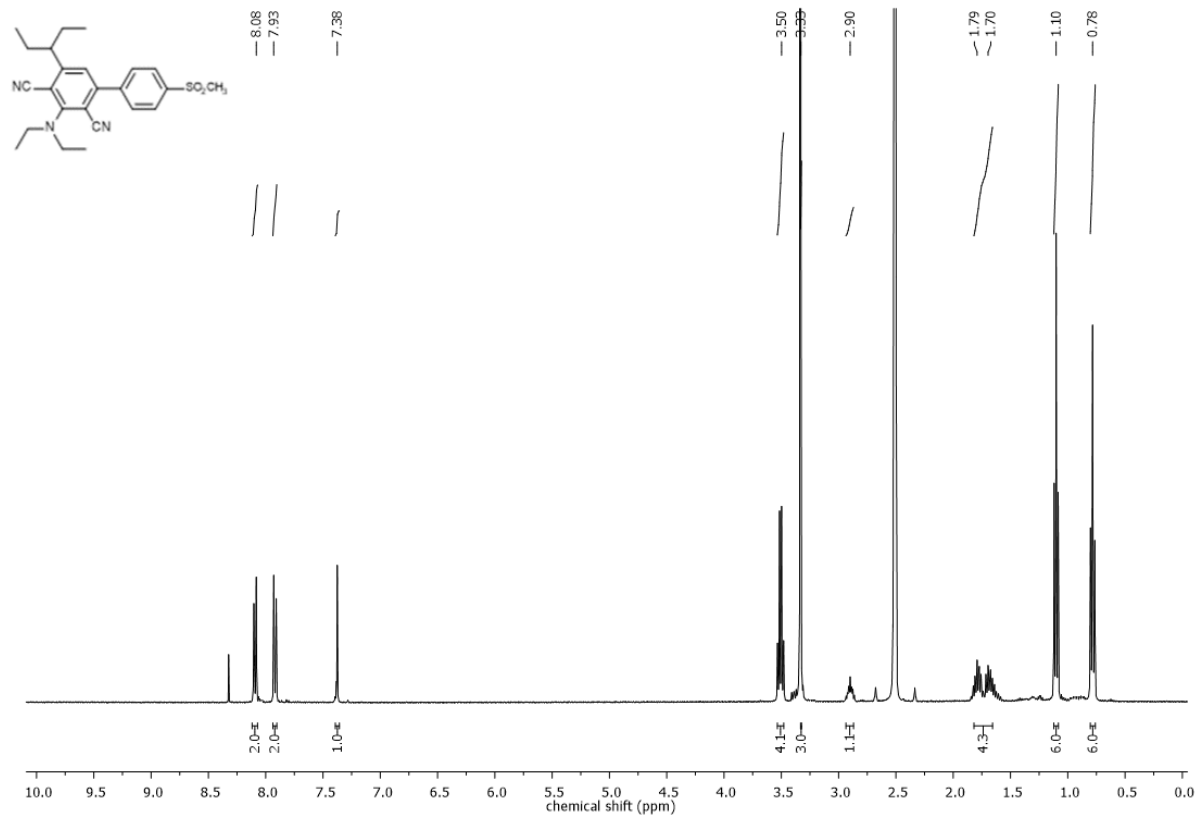


**Figure S9.** $^{1}$HNMR of 2-(diethylamino)-4-(1-ethylpropyl)-6-(4-methylsulfonylphenyl)benzene-1,3-dicarbonitrile (**BI-PH-SO$_2$-CH$_3$**).

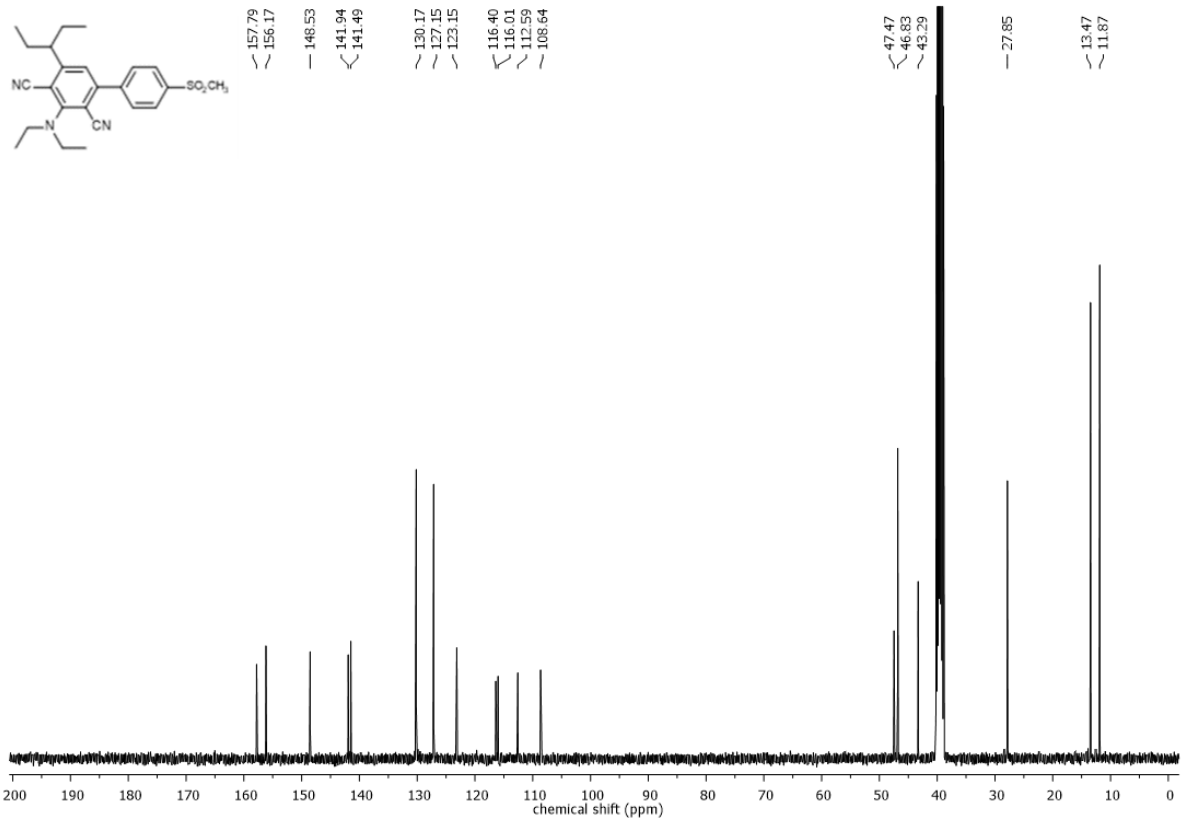


**Figure S10.** $^{13}$CNMR of 2-(diethylamino)-4-(1-ethylpropyl)-6-(4-methylsulfonylphenyl)benzene-1,3-dicarbonitrile (**BI-PH-SO$_2$-CH$_3$**).

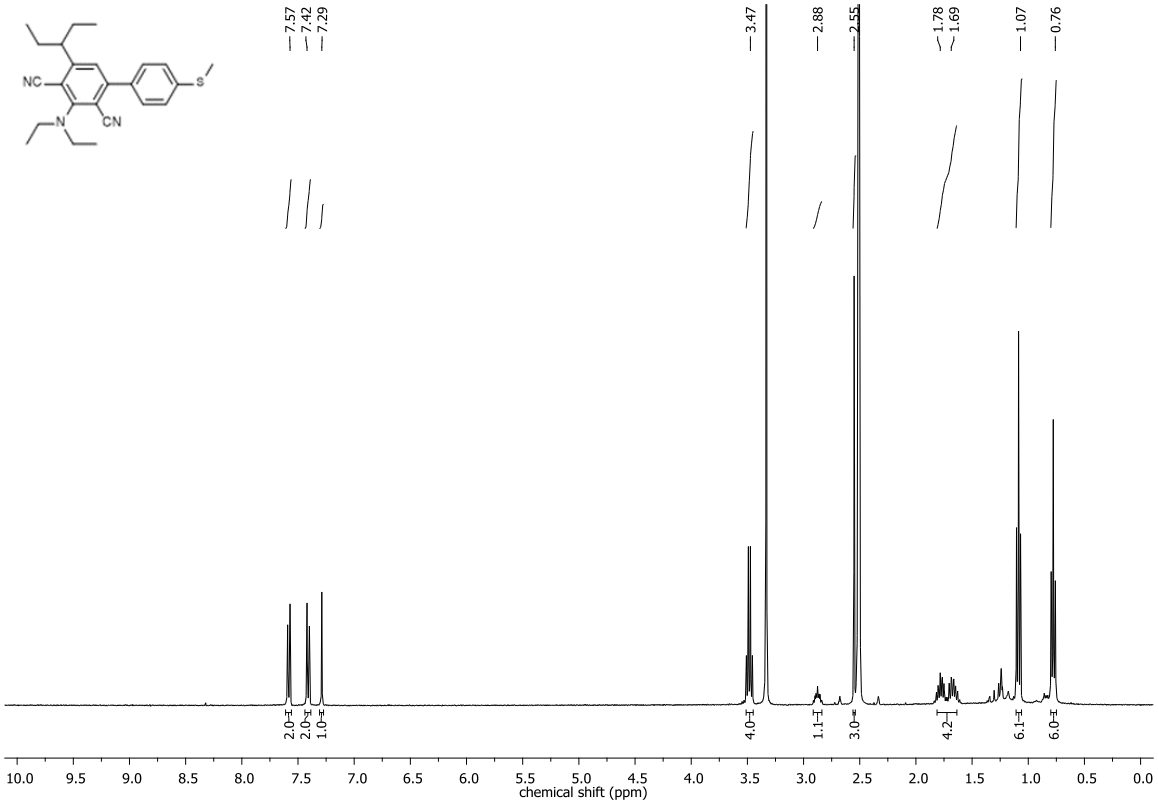


**Figure S11.** $^{1}$HNMR of 2-(diethylamino)-4-(1-ethylpropyl)-6-(4-methylsulfanylphenyl)benzene-1,3-dicarbonitrile (**BI-PH-S-CH$_3$**).

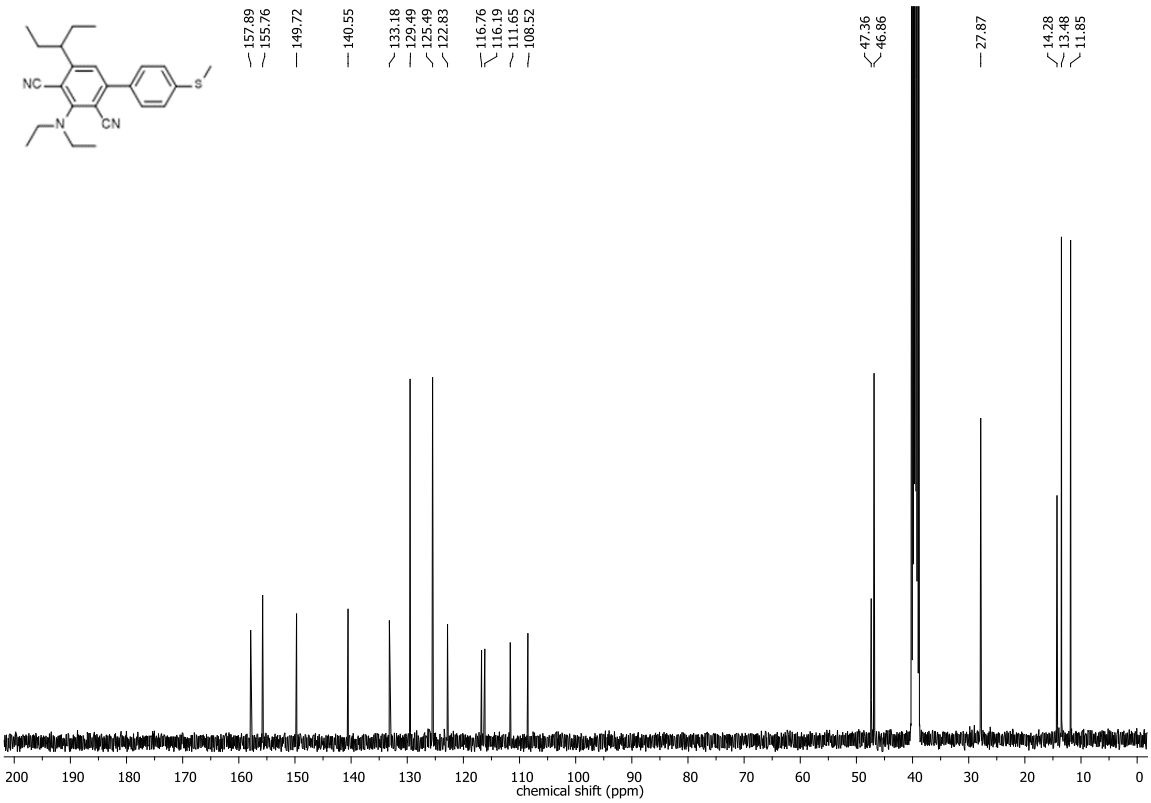


**Figure S12.** $^{13}$CNMR of 2-(diethylamino)-4-(1-ethylpropyl)-6-(4-methylsulfanylphenyl)benzene-1,3-dicarbonitrile (**BI-PH-S-CH$_3$**).

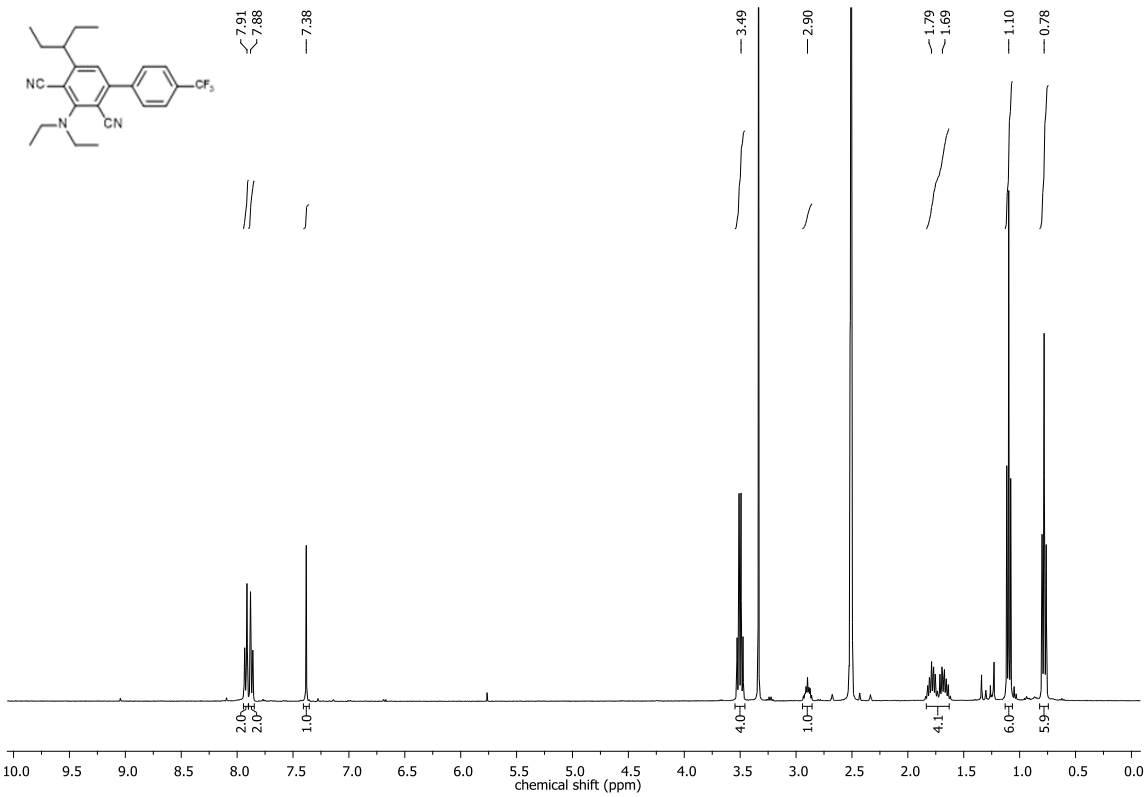


**Figure S13.** $^{1}$HNMR of 2-(diethylamino)-4-(1-ethylpropyl)-6-[4-(trifluoromethyl)phenyl]benzene-1,3-dicarbonitrile (**BI-PH-CF$_3$**).

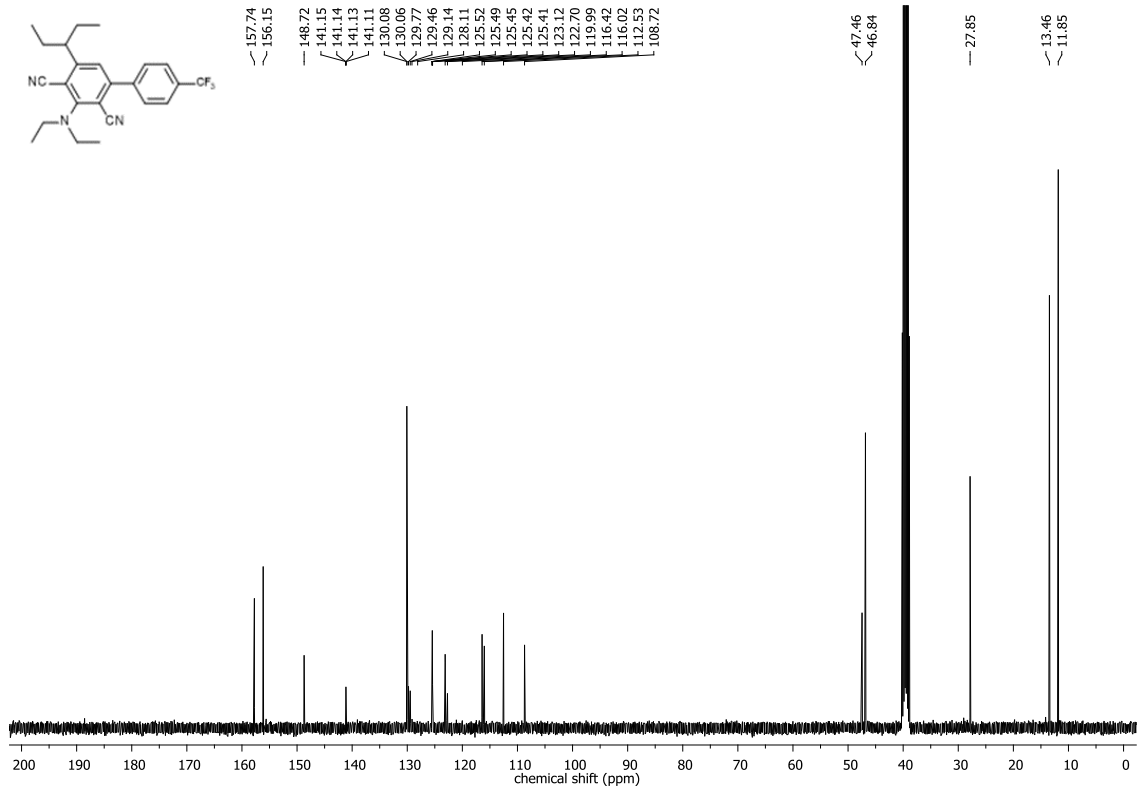


**Figure 14.** $^{13}$CNMR of 2-(diethylamino)-4-(1-ethylpropyl)-6-[4-(trifluoromethyl)phenyl]benzene-1,3-dicarbonitrile (**BI-PH-CF$_3$**).

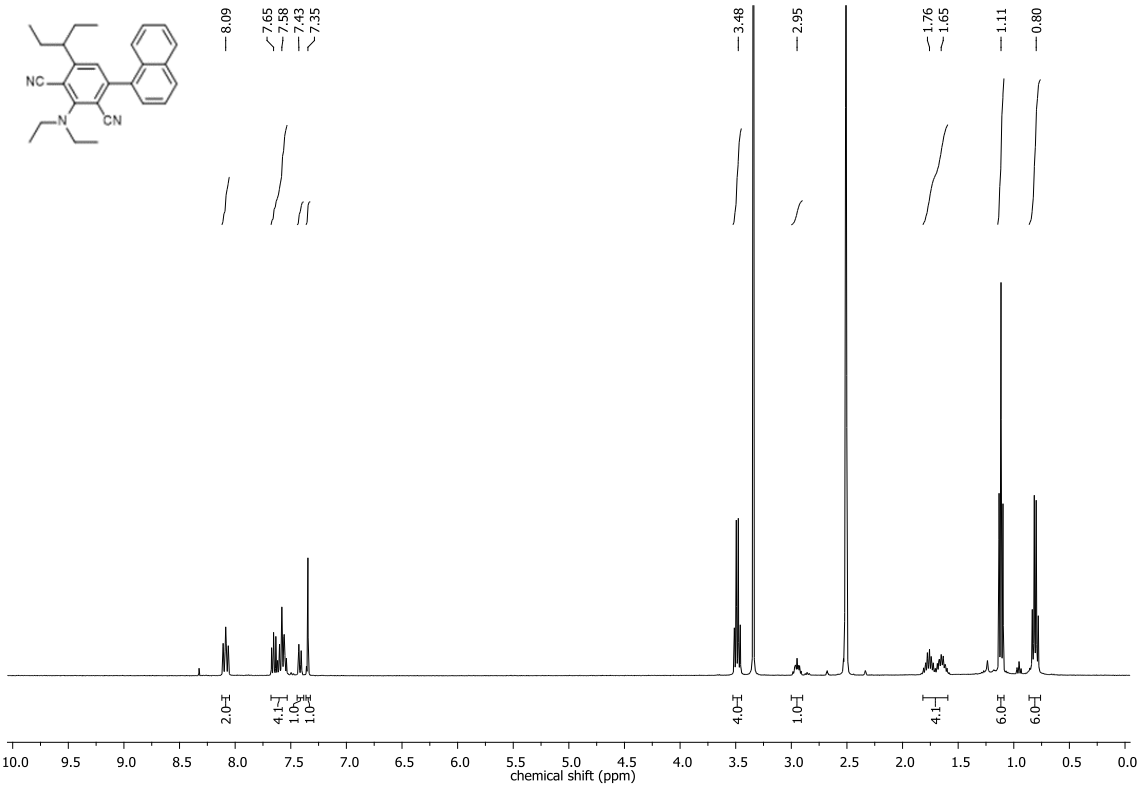


**Figure S15.** $^{1}$HNMR of 2-(diethylamino)-4-(1-ethylpropyl)-6-(1-naphthyl)benzene-1,3-dicarbonitrile (**BI-1-NPH**).

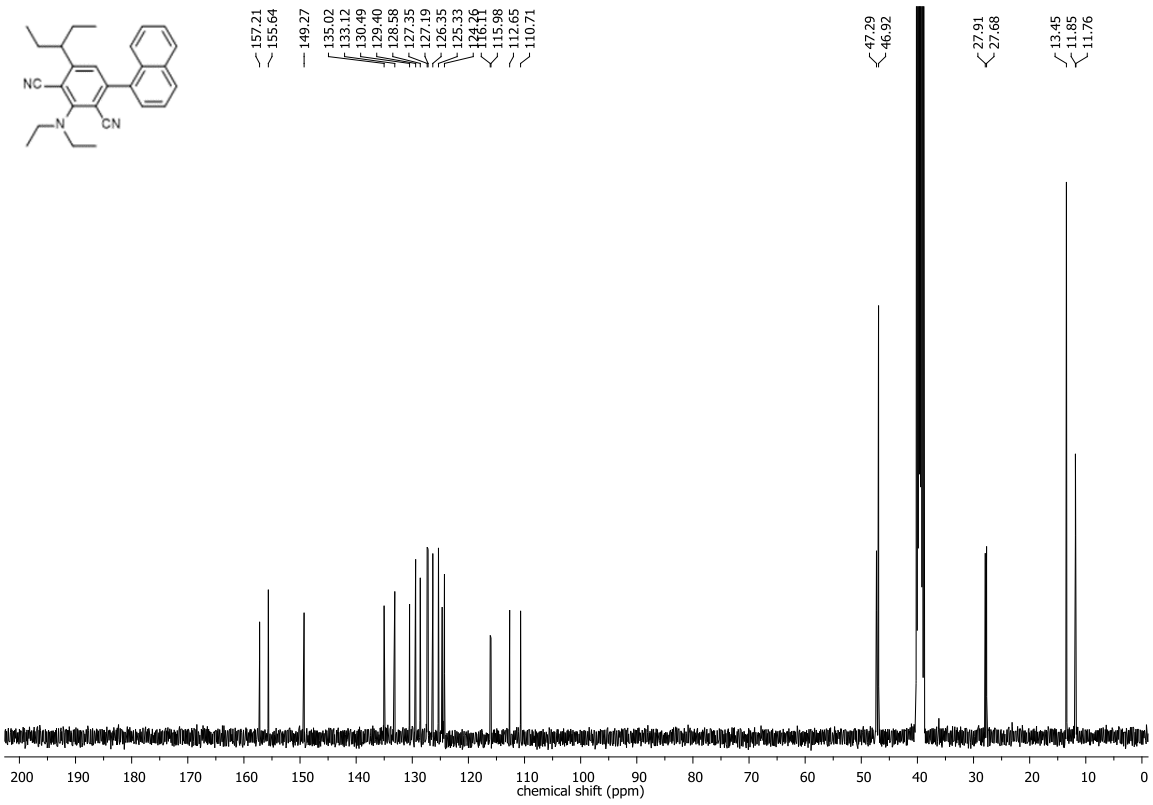


**Figure S16.** $^{13}$CNMR of 2-(diethylamino)-4-(1-ethylpropyl)-6-(1-naphthyl)benzene-1,3-dicarbonitrile (**BI-1-NPH**).

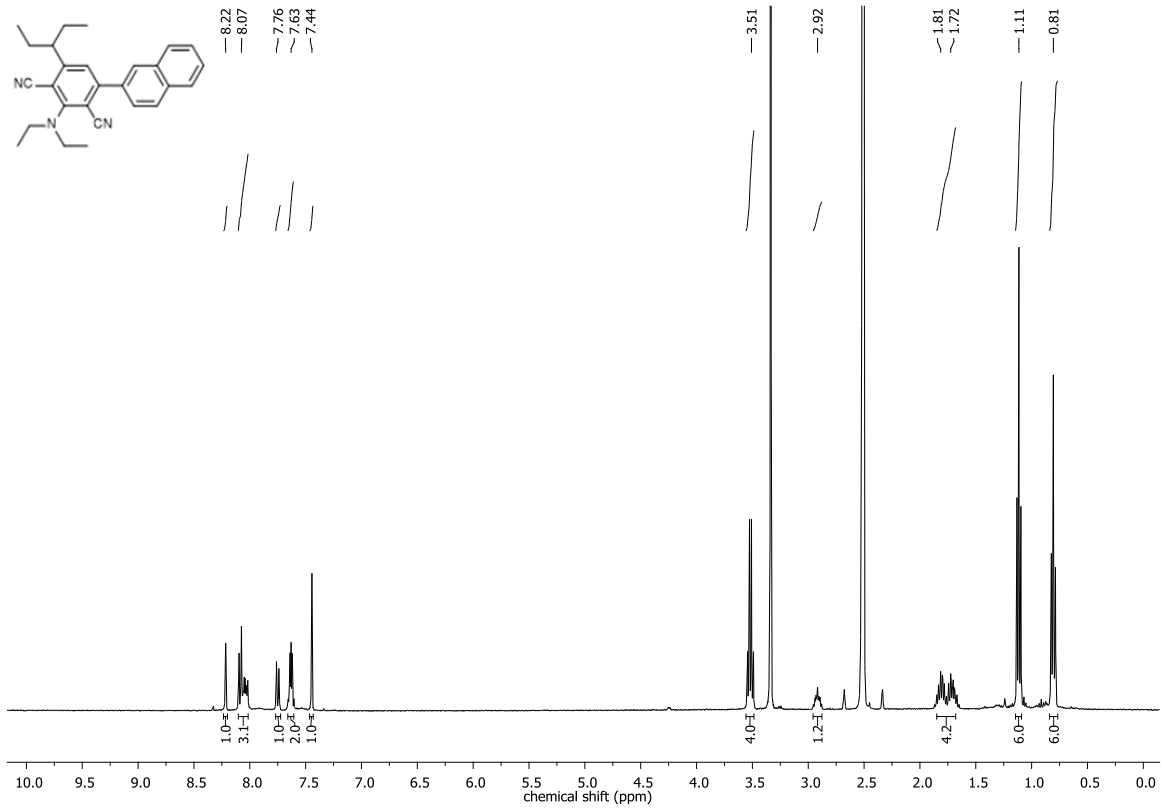


**Figure S17.** [1]HNMR of 2-(diethylamino)-4-(1-ethylpropyl)-6-(2-naphthyl)benzene-1,3-dicarbonitrile (**BI-2-NPH**).

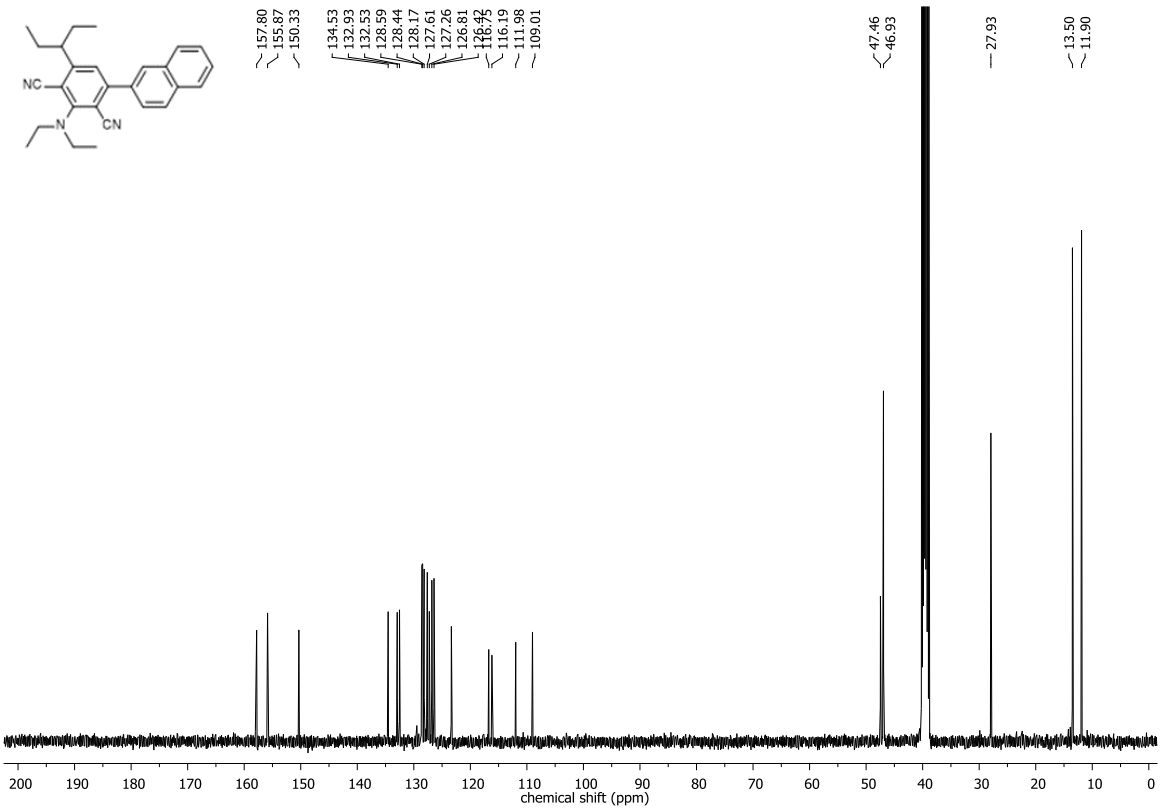


**Figure S18.** [13]CNMR of 2-(diethylamino)-4-(1-ethylpropyl)-6-(2-naphthyl)benzene-1,3-dicarbonitrile (**BI-2-NPH**).

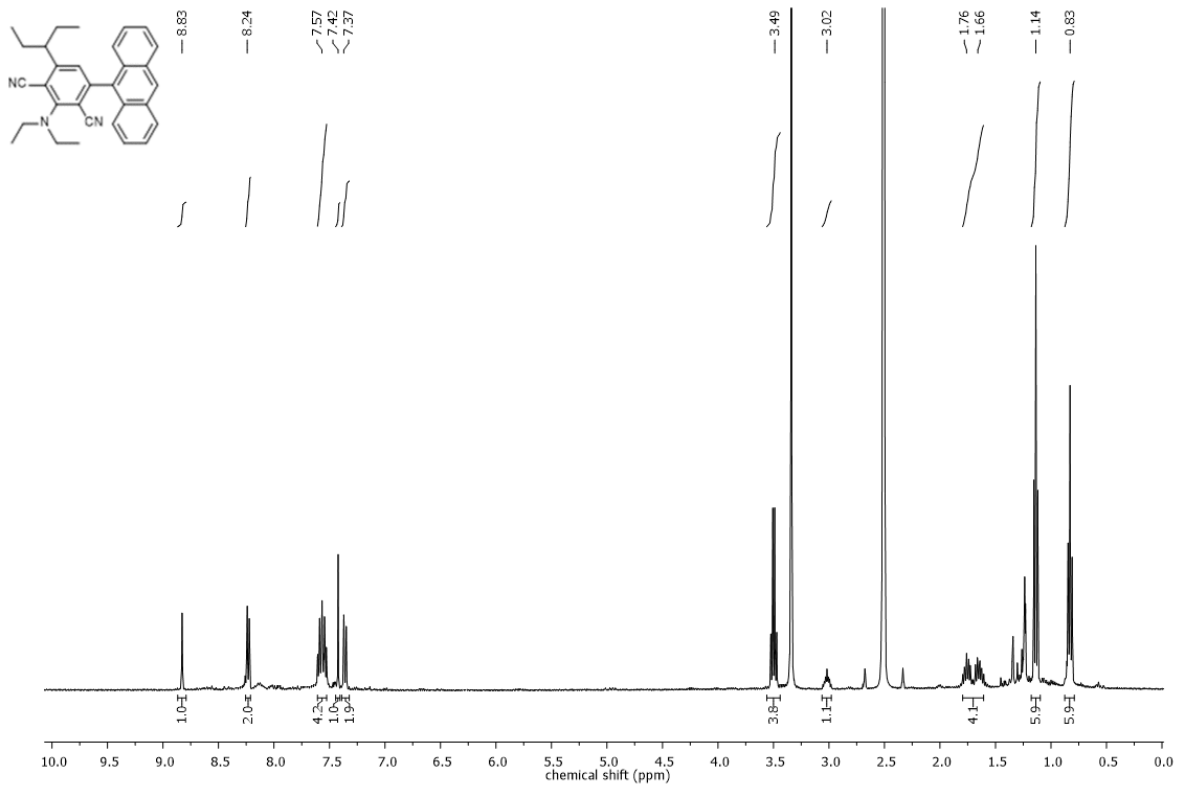


**Figure S19.** $^{1}$HNMR of 4-(9-anthryl)-2-(diethylamino)-6-(1-ethylpropyl)benzene-1,3-dicarbonitrile (**BI-1-AN**).

## Structure of compounds used in this study

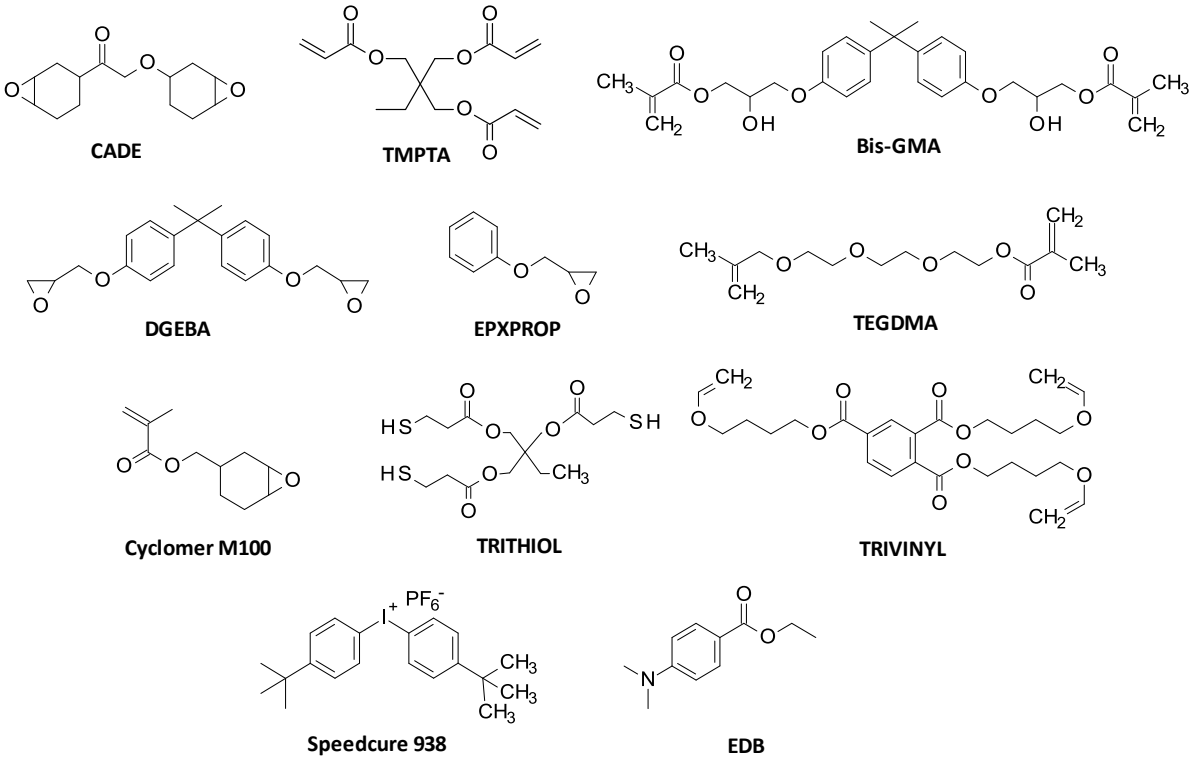


**Figure S20.** Structure of compounds used in the study.

## Cyclic voltammetry curves showing oxidation and reduction processes of 2-(diethylamino)-4-methyl-6-phenyl-benzene-1,3-dicarbonitrile derivatives in acetonitrile.

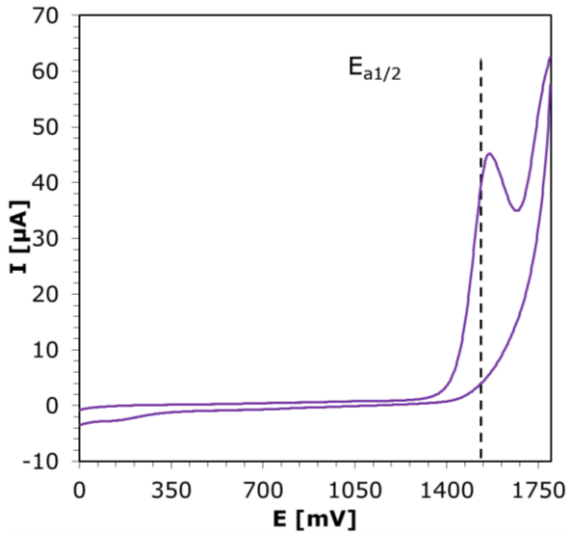


**Figure S21:** Cyclic voltammogram curves of the BI-PH oxidation in acetonitrile.

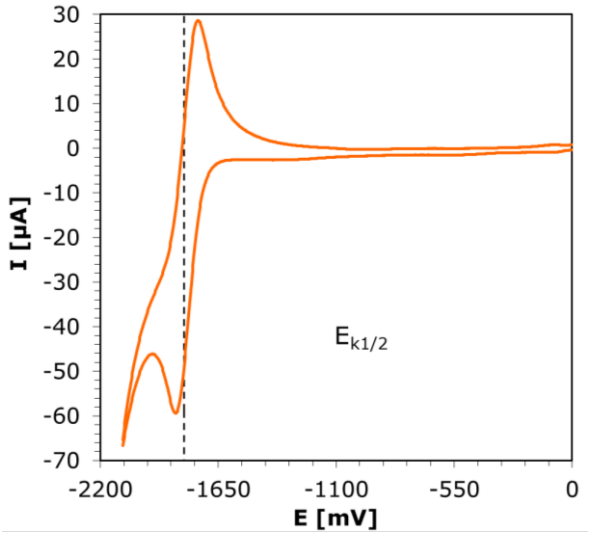


**Figure S22:** Cyclic voltammogram curves of the BI-PH reduction in acetonitrile.

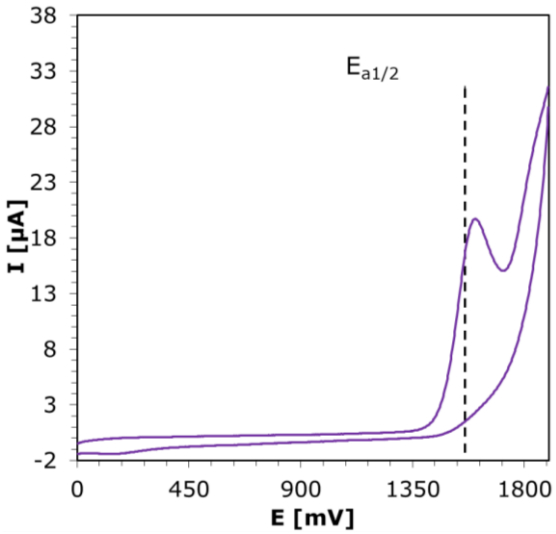


**Figure S23:** Cyclic voltammogram curves of the BI-PH-$CH_3$ oxidation in acetonitrile.

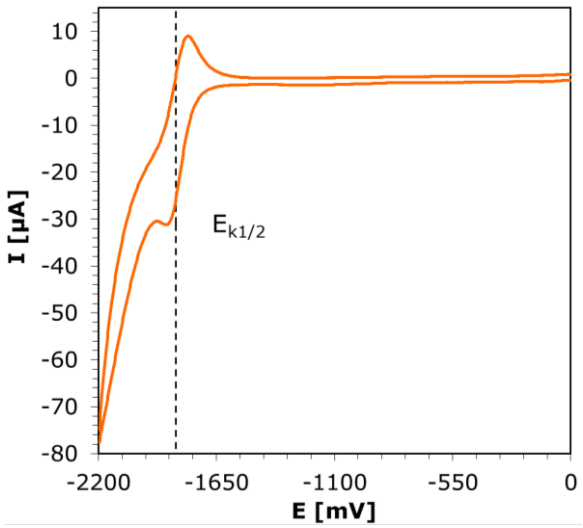


**Figure S24:** Cyclic voltammogram curves of the BI-PH-$CH_3$ reduction in acetonitrile.

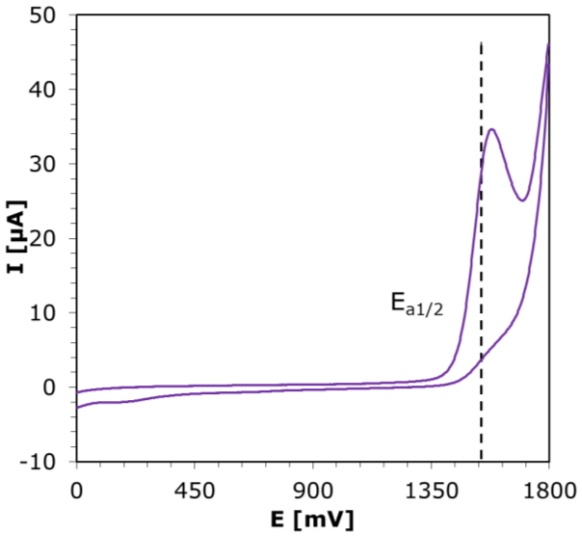


**Figure S25:** Cyclic voltammogram curves of the BI-PH-O-$CH_3$ oxidation in acetonitrile.

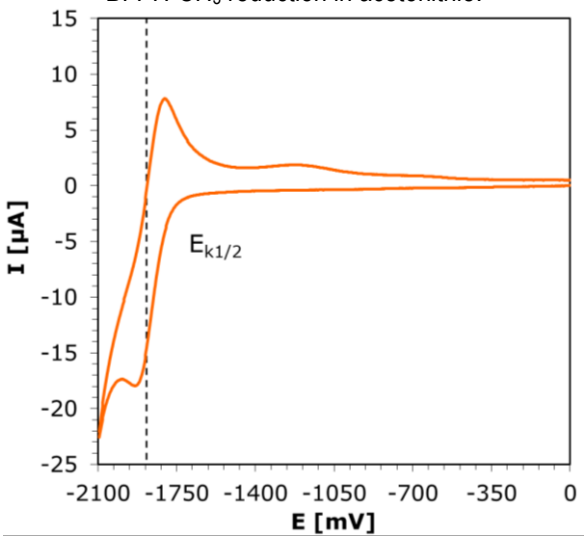


**Figure S26:** Cyclic voltammogram curves of the BI-PH-O-$CH_3$ reduction in acetonitrile.

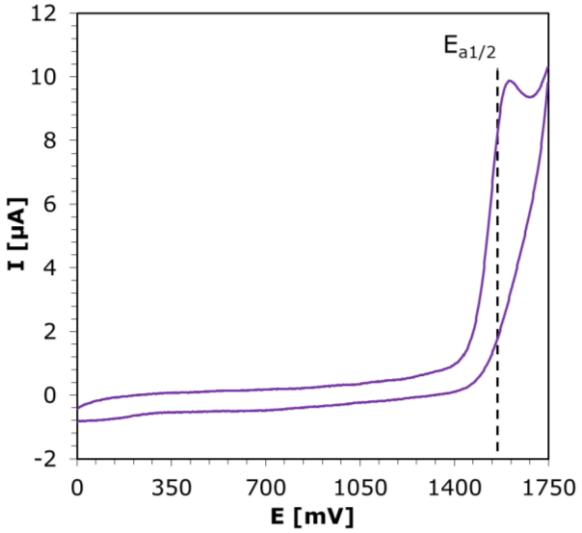


**Figure S27:** Cyclic voltammogram curves of the BI-PH-CN oxidation in acetonitrile.

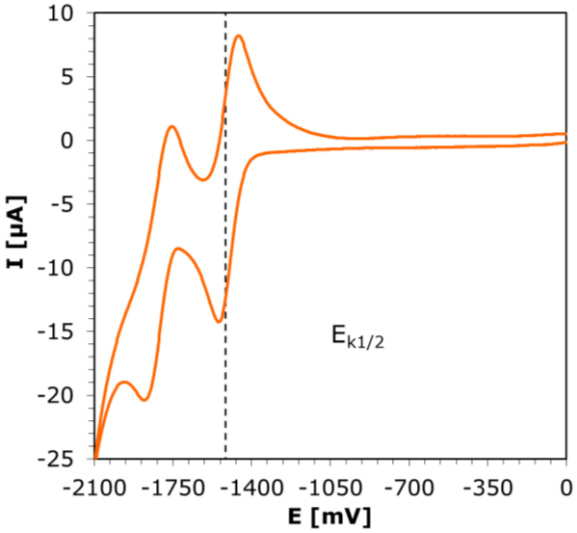


**Figure S28:** Cyclic voltammogram curves of the BI-PH-CN reduction in acetonitrile.

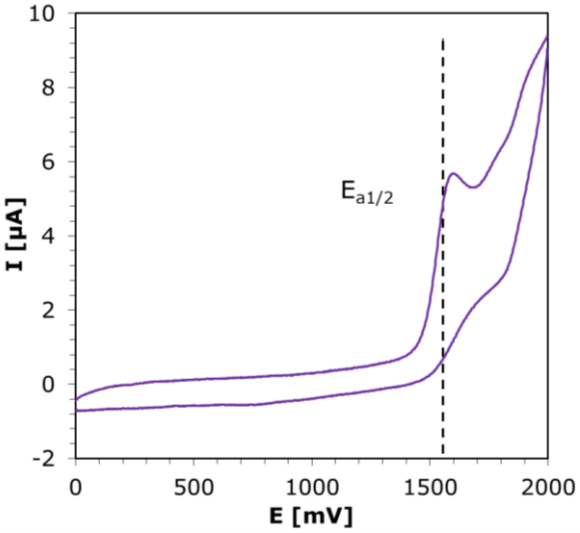


**Figure S29:** Cyclic voltammogram curves of the BI-PH-$SO_2$-$CH_3$ oxidation in acetonitrile.

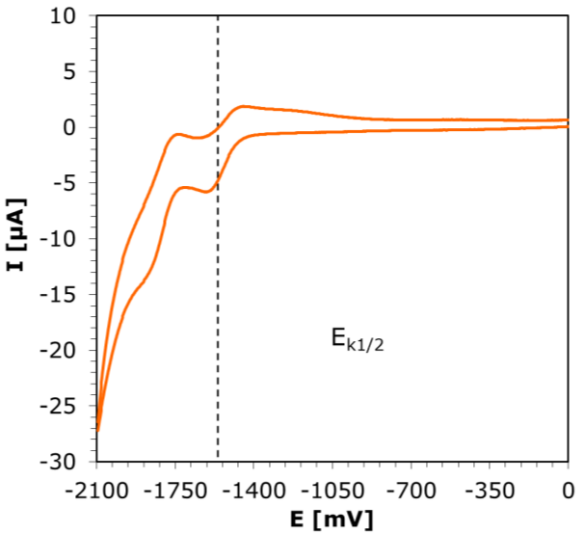


**Figure S30:** Cyclic voltammogram curves of the BI-PH-$SO_2$-$CH_3$ reduction in acetonitrile.

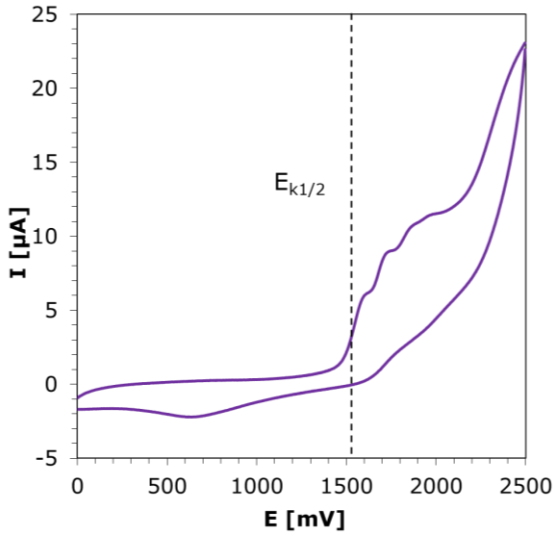


**Figure S31:** Cyclic voltammogram curves of the BI-PH-S-$CH_3$ oxidation in acetonitrile.

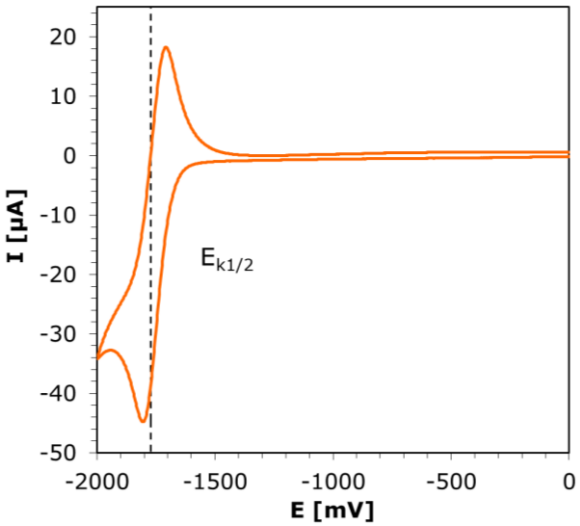


**Figure S32:** Cyclic voltammogram curves of the BI-PH-S-$CH_3$ reduction in acetonitrile.

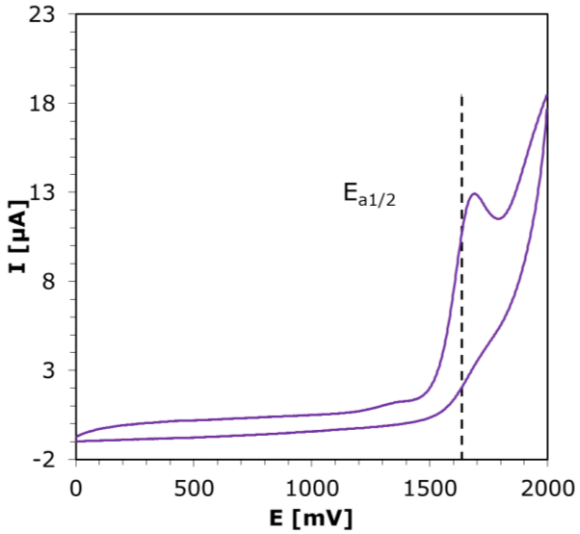


**Figure S33:** Cyclic voltammogram curves of the BI-PH-$CF_3$ oxidation in acetonitrile.

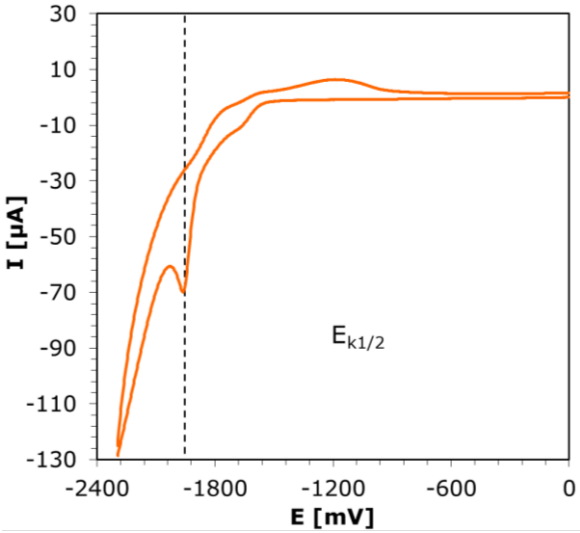


**Figure S34:** Cyclic voltammogram curves of the BI-PH-$CF_3$ reduction in acetonitrile.

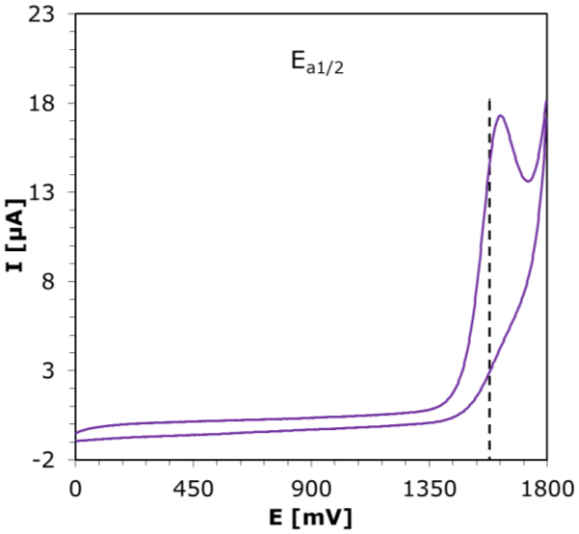


**Figure S35:** Cyclic voltammogram curves of the BI-1-NPH oxidation in acetonitrile.

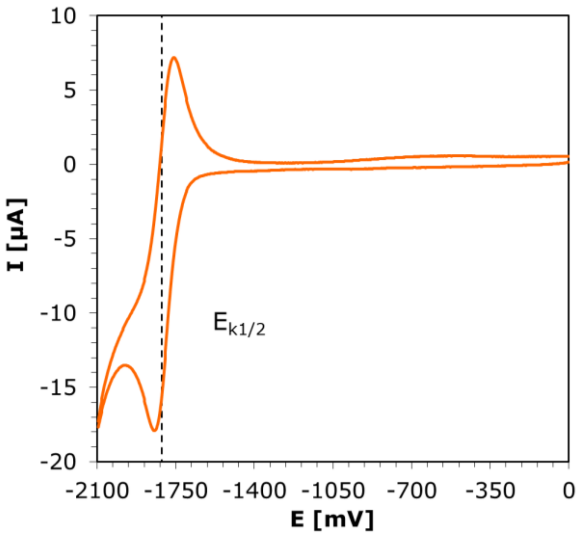


**Figure S36:** Cyclic voltammogram curves of the BI-1-NPH reduction in acetonitrile.

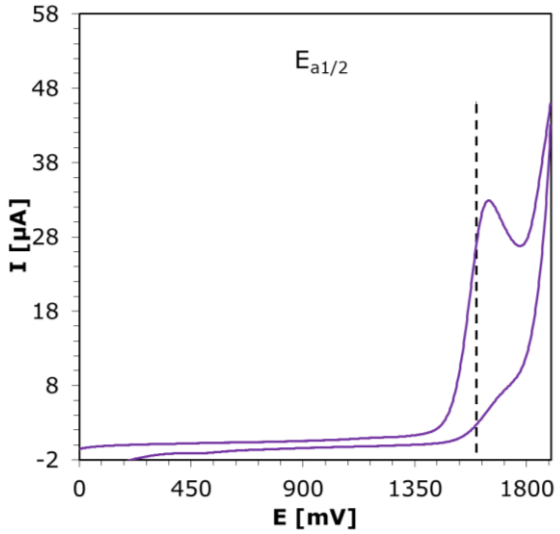


**Figure S37:** Cyclic voltammogram curves of the BI-2-NPH oxidation in acetonitrile.

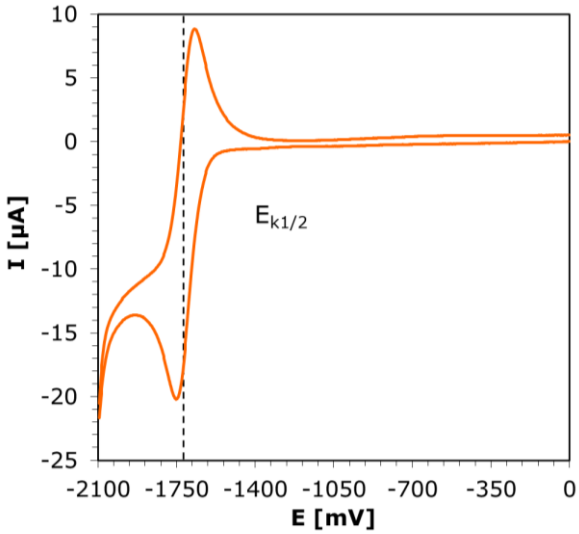


**Figure S38:** Cyclic voltammogram curves of the BI-2-NPH reduction in acetonitrile.

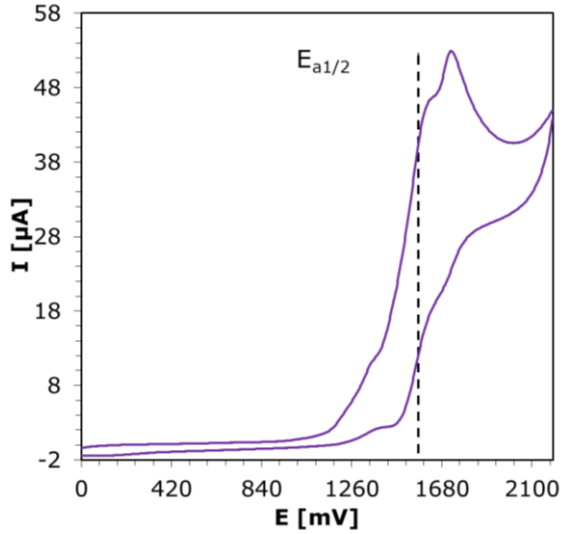


**Figure S39:** Cyclic voltammogram curves of the BI-1-AN oxidation in acetonitrile.

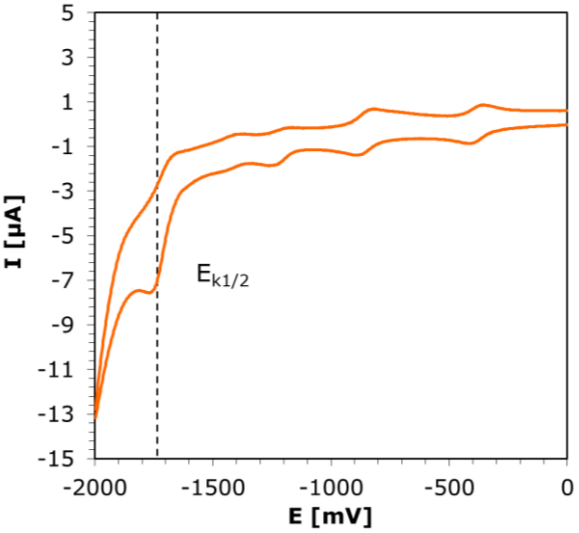


**Figure S40:** Cyclic voltammogram curves of the BI-1-AN reduction in acetonitrile.

**Absorption and fluorescence spectra for the determination of the excited singlet state energy for investigated of 2-(diethylamino)-4-methyl-6-phenyl-benzene-1,3-dicarbonitrile derivatives in acetonitrile.**

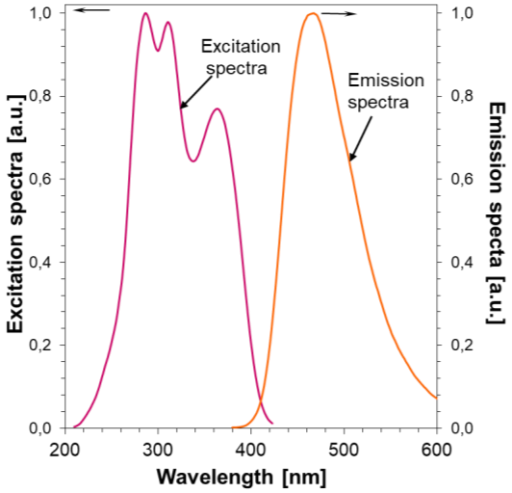


**Figure S41:** Excitation and emission spectra for the determination of the excited singlet state energy for BI-PH derivative.

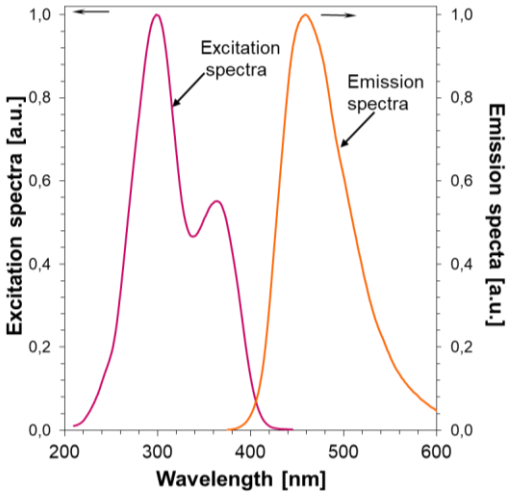


**Figure S42:** Excitation and emission spectra for the determination of the excited singlet state energy for BI-PH-$CH_3$ derivative.

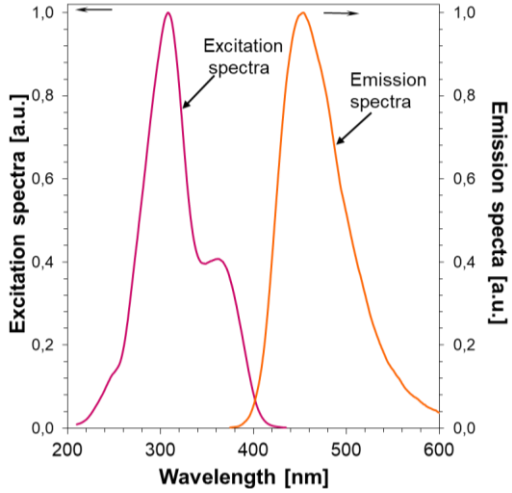


**Figure S43:** Excitation and emission spectra for the determination of the excited singlet state energy for BI-PH-O-$CH_3$ derivative.

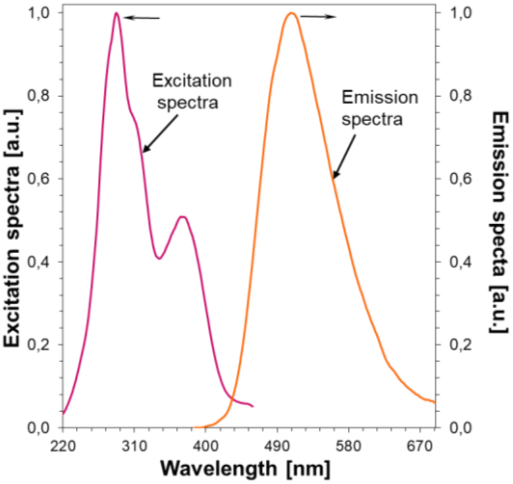


**Figure S44:** Excitation and emission spectra for the determination of the excited singlet state energy for BI-PH-CN derivative.

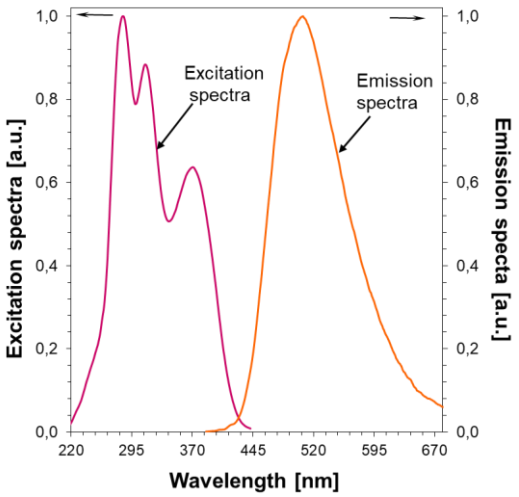


**Figure S45:** Excitation and emission spectra for the determination of the excited singlet state energy for BI-PH-$SO_2$-$CH_3$ derivative.

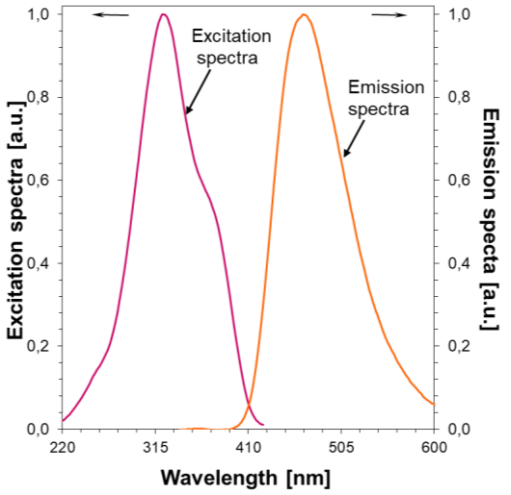


**Figure S46:** Excitation and emission spectra for the determination of the excited singlet state energy for BI-PH-S-$CH_3$ derivative.

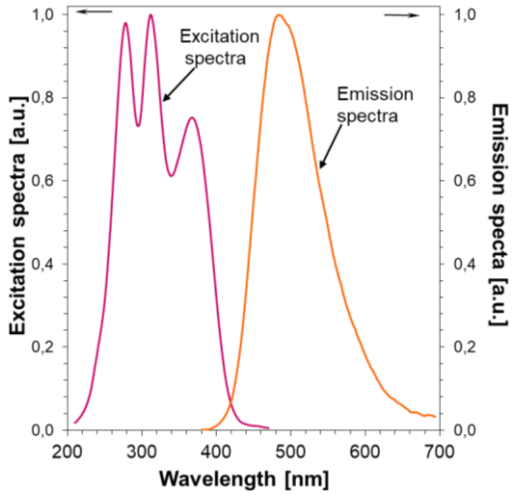


**Figure S47:** Excitation and emission spectra for the determination of the excited singlet state energy for BI-PH-$CF_3$ derivative.

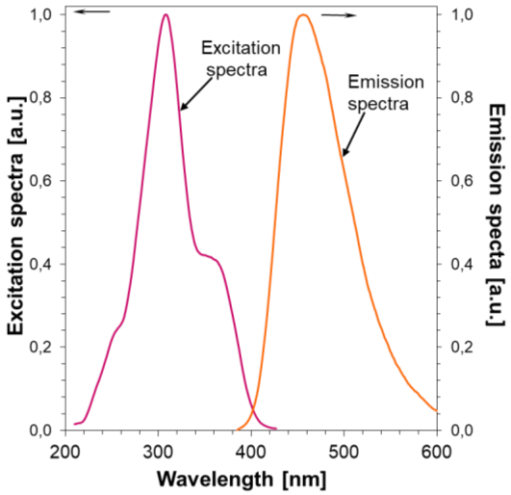


**Figure S48:** Excitation and emission spectra for the determination of the excited singlet state energy for BI-1-NPH derivative.

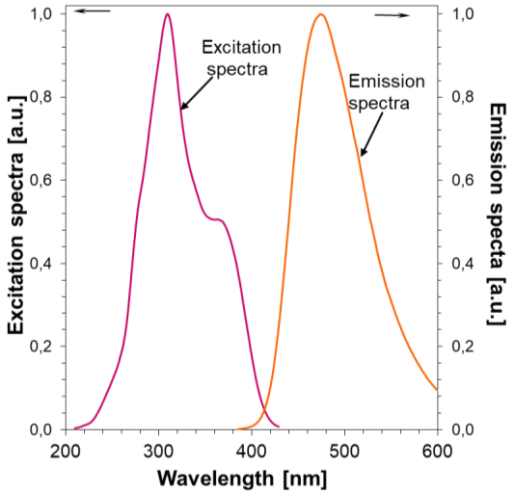


**Figure S49:** Excitation and emission spectra for the determination of the excited singlet state energy for BI-2-NPH derivative.

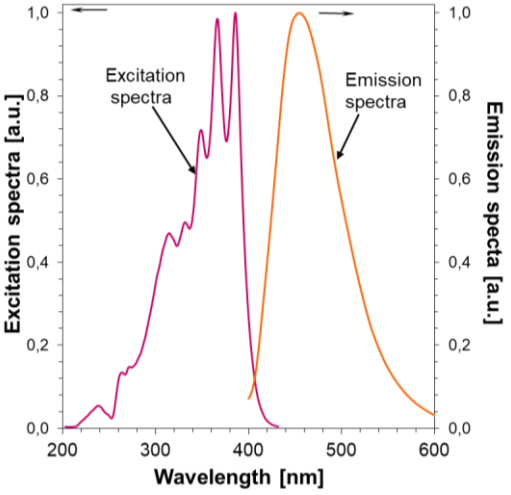


**Figure S50:** Excitation and emission spectra for the determination of the excited singlet state energy for BI-1-AN derivative.

**The optimized structures and HOMO and LUMO orbitals of investigated 2-(diethylamino)-4-**

**methyl-6-phenyl-benzene-1,3-dicarbonitrile derivatives free molecules determined with the use of uB3LYP/6-31G* level of theory**

| Compound | HOMO | LUMO |
|---|---|---|
| **BI-PH**<br> 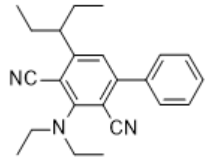 <br>*2-(diethylamino)-4-(1-ethylpropyl)-6-phenylbenzene-1,3-dicarbonitrile* | 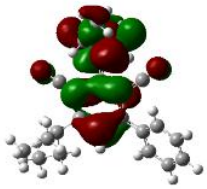 | 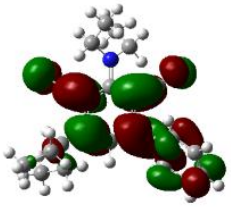 |
| **BI-PH-$CH_3$**<br> 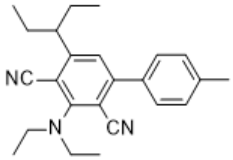 <br>*2-(diethylamino)-4-(1-ethylpropyl)-6-(4-methylphenyl)benzene-1,3-dicarbonitrile* | 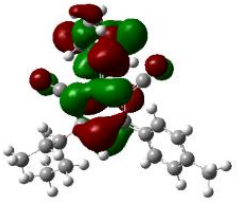 | 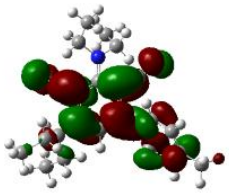 |
| **BI-PH-O-$CH_3$**<br> 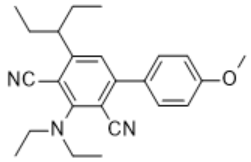 <br>*2-(diethylamino)-6-(1-ethylpropyl)-4-(4-methoxyphenyl) benzene-1,3-dicarbonitrile* | 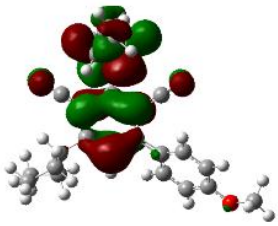 | 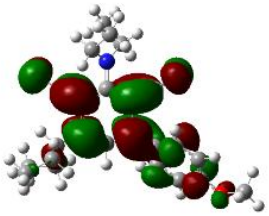 |
| **BI-PH-CN**<br> 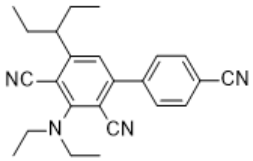 <br>*4-(4-cyanophenyl)-2-(diethylamino)-6-(1-ethylpropyl)benzene-1,3-dicarbonitrile* | 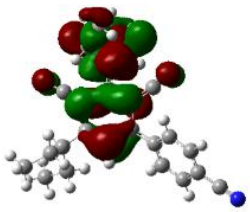 | 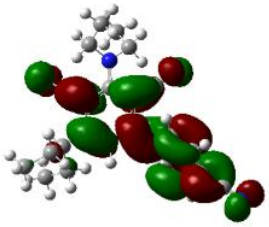 |
| **BI-PH-$SO_2$-$CH_3$**<br> 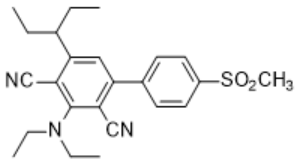 <br>*2-(diethylamino)-4-(1-ethylpropyl)-6-(4-methylsulfonylphenyl)benzene-1,3-dicarbonitrile* | 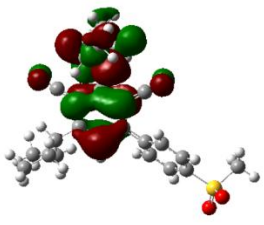 | 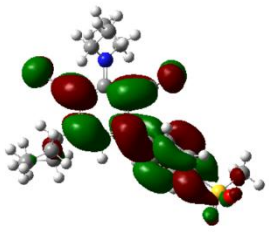 |

| | | |
|---|---|---|
| **BI-PH-S-CH$_3$**<br> 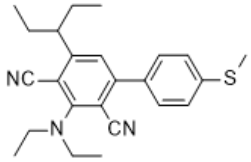 <br>*2-(diethylamino)-4-(1-ethylpropyl)-6-(4-methylsulfanylphenyl)benzene-1,3-dicarbonitrile* | 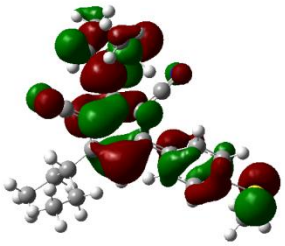 | 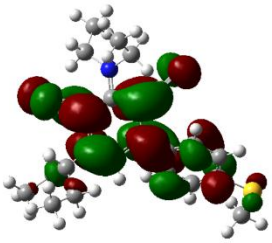 |
| **BI-PH-CF$_3$**<br> 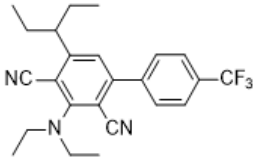 <br>*2-(diethylamino)-4-(1-ethylpropyl)-6-[4-(trifluoromethyl)phenyl]benzene-1,3-dicarbonitrile* | 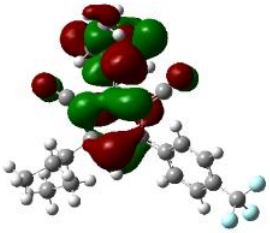 | 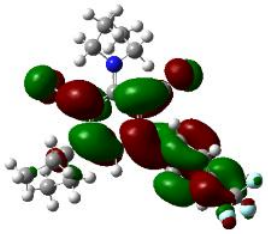 |
| **BI-1-NPH**<br> 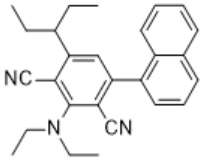 <br>*2-(diethylamino)-4-(1-ethylpropyl)-6-(1-naphthyl)benzene-1,3-dicarbonitrile* | 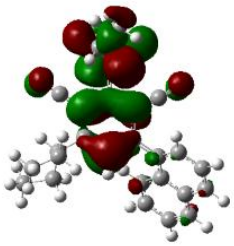 | 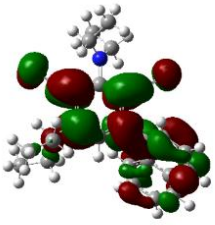 |
| **BI-2-NPH**<br> 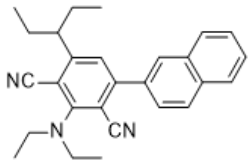 <br>*2-(diethylamino)-4-(1-ethylpropyl)-6-(2-naphthyl)benzene-1,3-dicarbonitrile* | 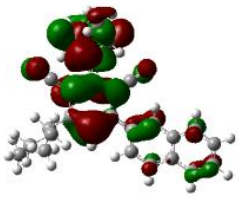 | 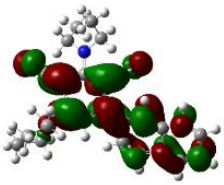 |
| **BI-1-AN**<br> 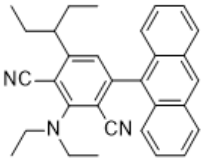 <br>*4-(9-anthryl)-2-(diethylamino)-6-(1-ethylpropyl)benzene-1,3-dicarbonitrile* | 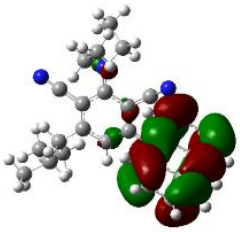 | 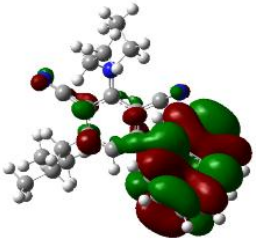 |

## Fluorescence quenching with Speedcure 938 (Iod) of investigated 2-(diethylamino)-4-methyl-6-phenyl-benzene-1,3-dicarbonitrile derivatives together with Stern-Volmer correlation

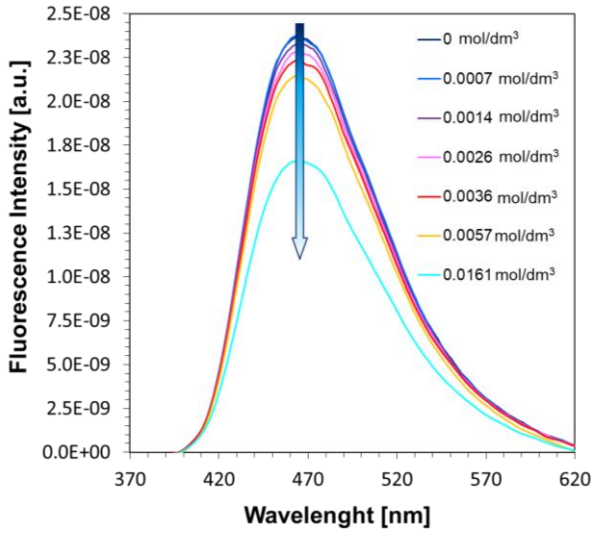


**Figure S51:** Fluorescence quenching of BI-PH.

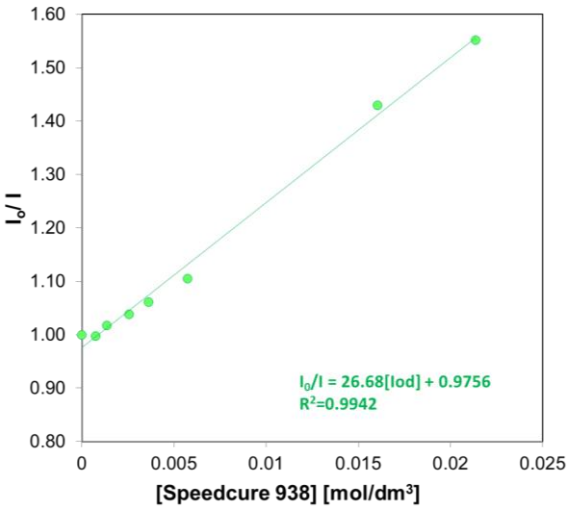


**Figure S52:** Stern-Volmer plots for the fluorescence quenching of BI-PH by Iod. Solvent acetonitrile.

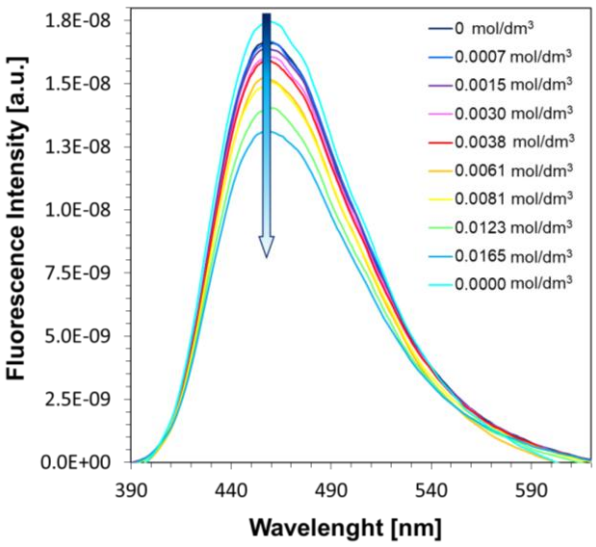


**Figure S53:** Fluorescence quenching of BI-PH-$CH_3$.

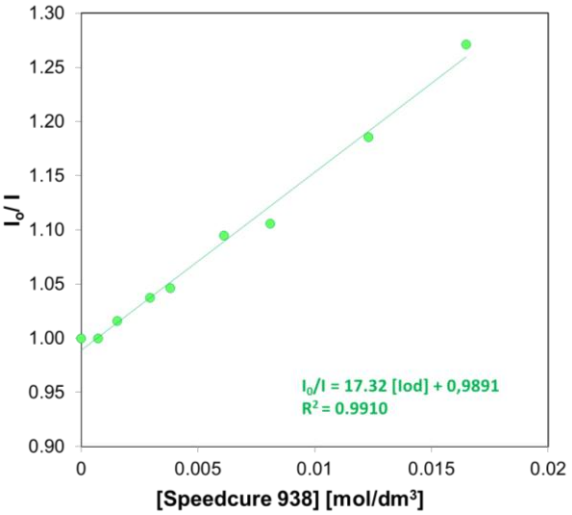


**Figure S54:** Stern-Volmer plots for the fluorescence quenching of BI-PH-$CH_3$ by Iod. Solvent acetonitrile.

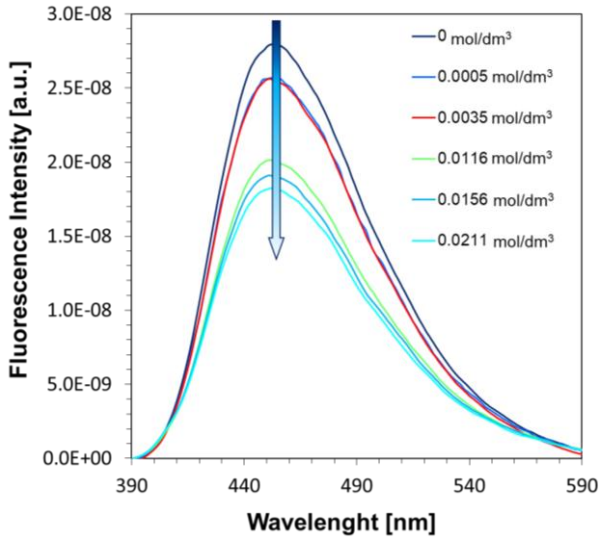


**Figure S55:** Fluorescence quenching of BI-PH-O-$CH_3$.

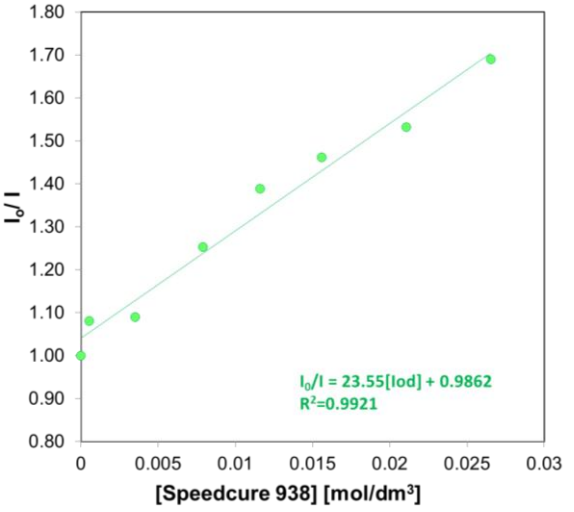


**Figure S56:** Stern-Volmer plots for the fluorescence

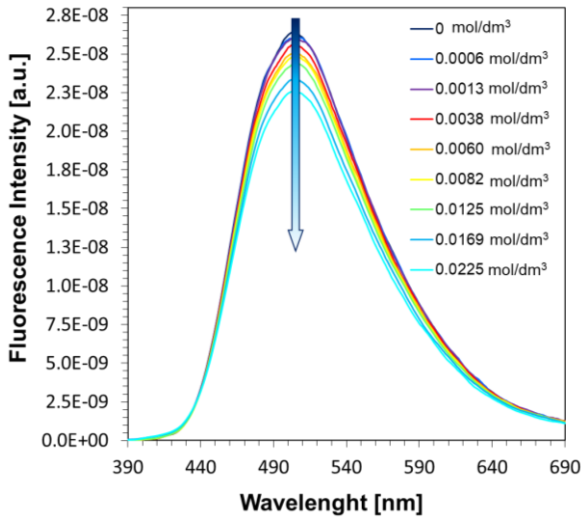


**Figure S587:** Fluorescence quenching of BI-PH-$SO_2$-$CH_3$.

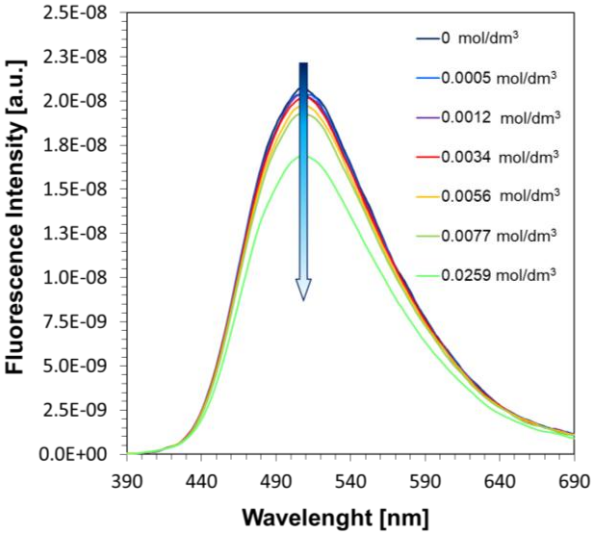


**Figure S59:** Fluorescence quenching of BI-PH-CN.

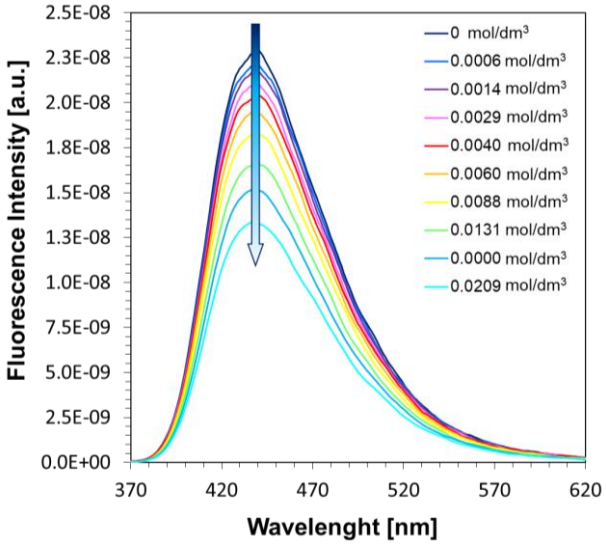


**Figure S61:** Fluorescence quenching of BI-PH-S-$CH_3$.

quenching of BI-PH-O-$CH_3$ by Iod. Solvent acetonitrile.

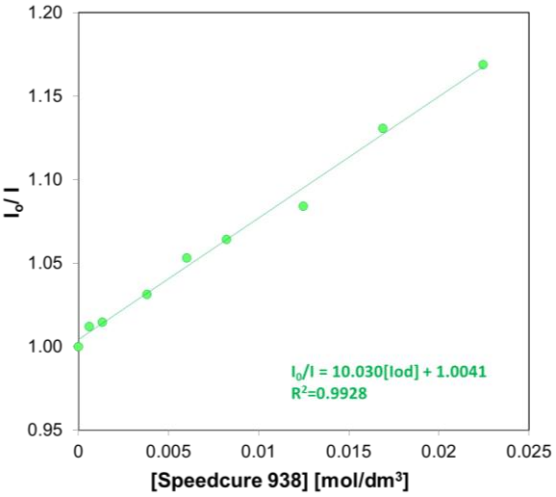


**Figure S58:** Stern-Volmer plots for the fluorescence quenching of BI-PH-$SO_2$-$CH_3$ by Iod. Solvent acetonitrile.

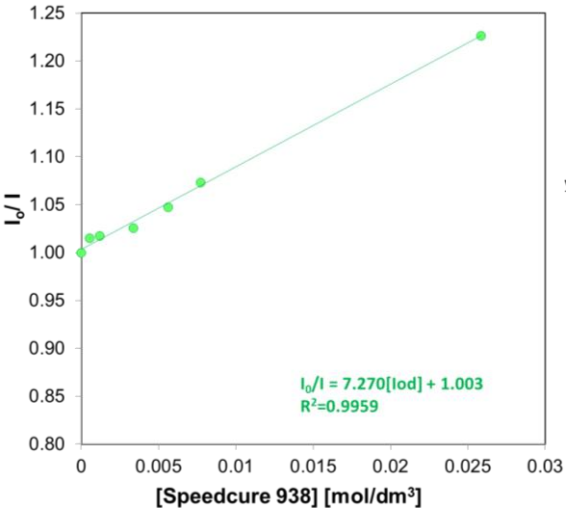


**Figure S60:** Stern-Volmer plots for the fluorescence quenching of BI-PH-CN by Iod. Solvent acetonitrile.

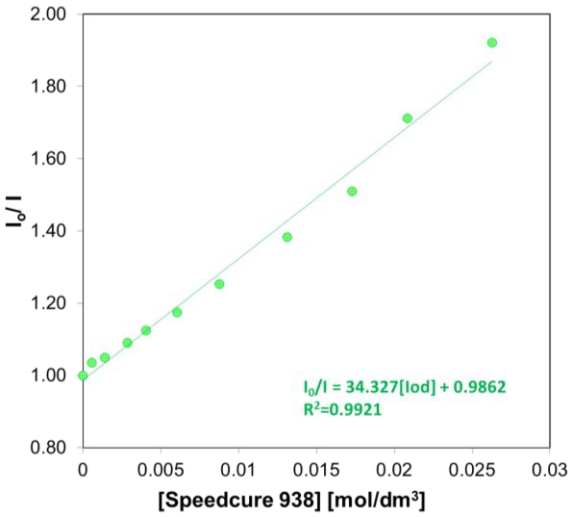


**Figure S62:** Stern-Volmer plots for the fluorescence quenching of BI-PH-S-$CH_3$ by Iod. Solvent acetonitrile.

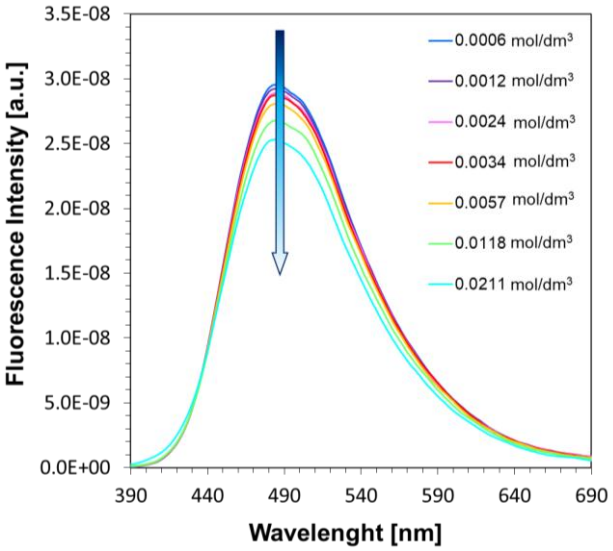


**Figure S63:** Fluorescence quenching of BI-PH-$CF_3$.

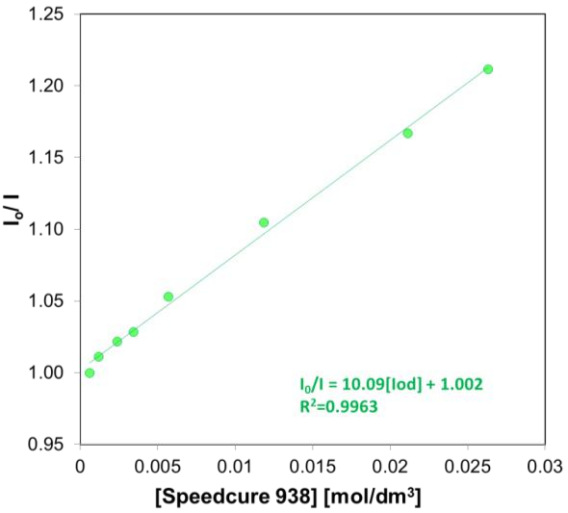


**Figure S64:** Stern-Volmer plots for the fluorescence quenching of BI-PH-$CF_3$ by Iod. Solvent acetonitrile.

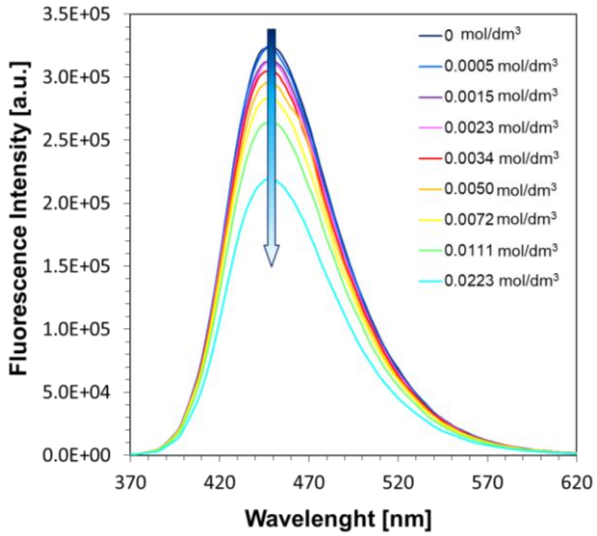


**Figure S65:** Fluorescence quenching of BI-1-NPH.

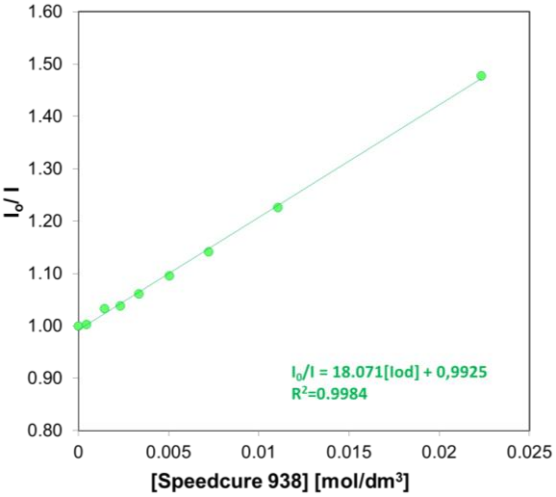


**Figure S66:** Stern-Volmer plots for the fluorescence quenching of BI-1-NPH by Iod. Solvent acetonitrile.

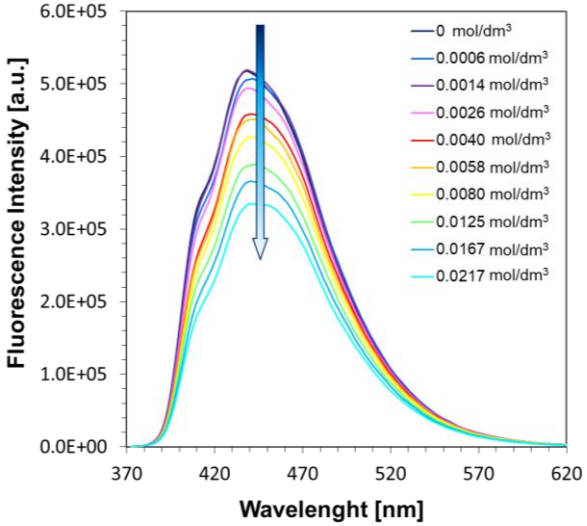


**Figure S67:** Fluorescence quenching of BI-2-NPH.

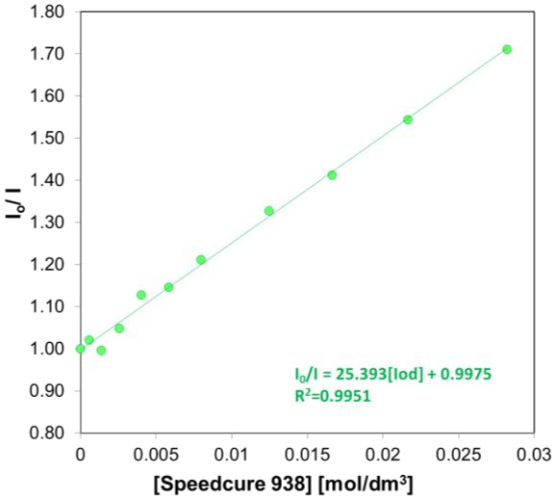


**Figure S68:** Stern-Volmer plots for the fluorescence quenching of BI-2-NPH by Iod. Solvent acetonitrile.

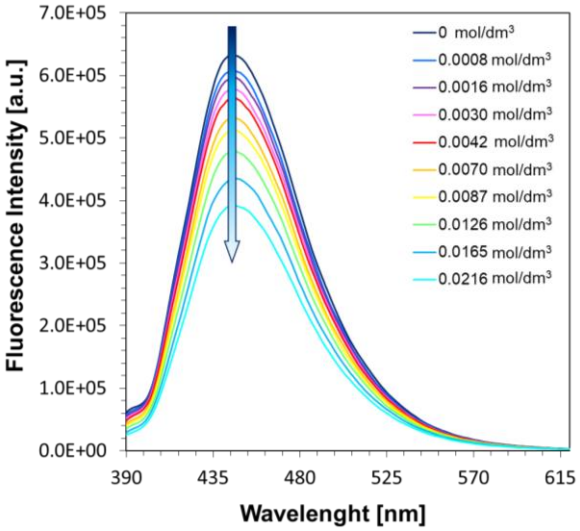


**Figure S69:** Fluorescence quenching of BI-1-AN.

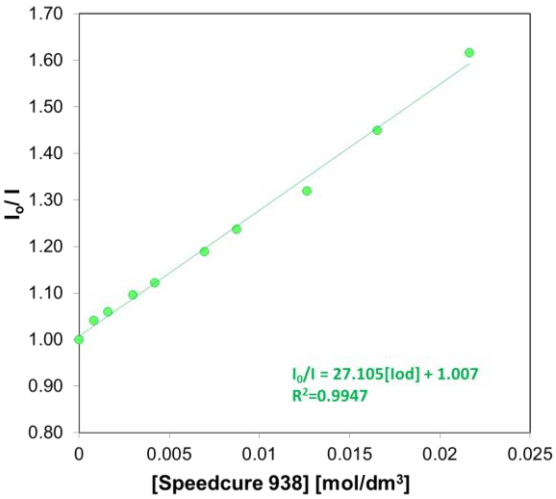


**Figure S70:** Stern-Volmer plots for the fluorescence quenching of BI-1-AN by Iod. Solvent acetonitrile.

## Steady state photolysis upon exposure with LED @365nm for 2-(diethylamino)-4-methyl-6-phenyl-benzene-1,3-dicarbonitrile derivatives in acetonitrile

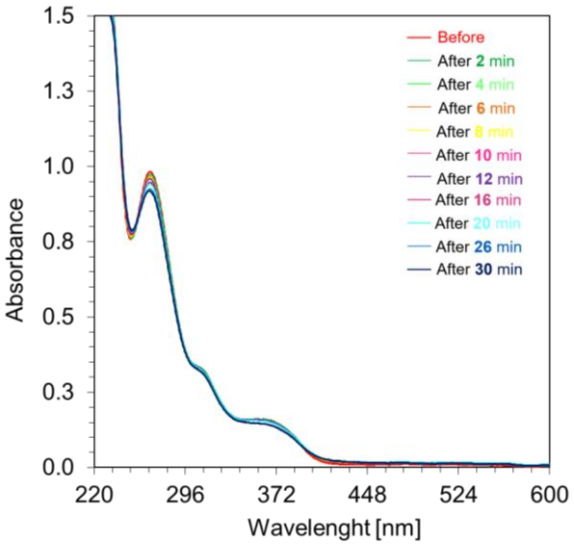


**Figure S71:** Photolysis of BI-PH in ACN under 365nm (190mW/cm$^2$).

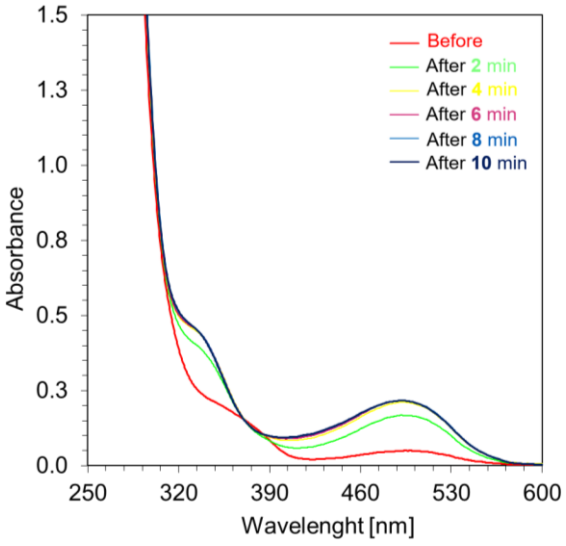


**Figure S72:** Photolysis of BI-PH + Speedcure 938 (concentration: 1,59·10$^{-3}$ [mol/dm$^3$]) in ACN under 365nm (190mW/cm$^2$).

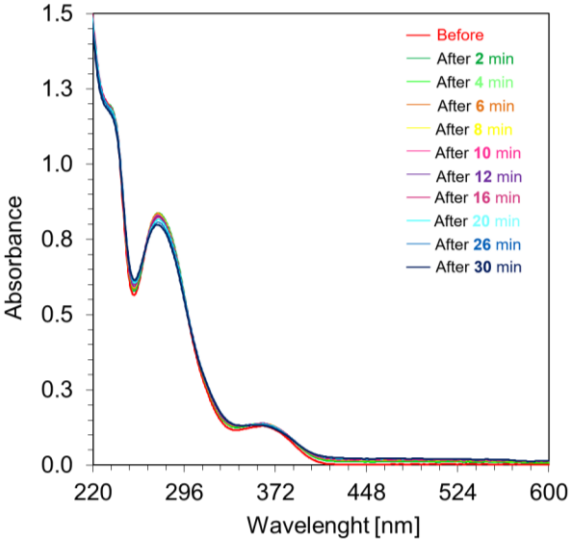


**Figure S73:** Photolysis of BI-PH-CH$_3$ in ACN under 365nm (190mW/cm$^2$).

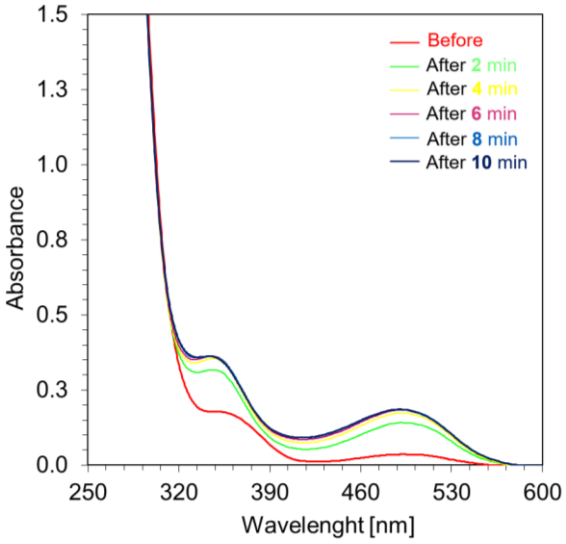


**Figure S74:** Photolysis of BI-PH-CH$_3$ + Speedcure 938 (concentration: 1,59·10$^{-3}$ [mol/dm$^3$]) in ACN under 365nm (190mW/cm$^2$).

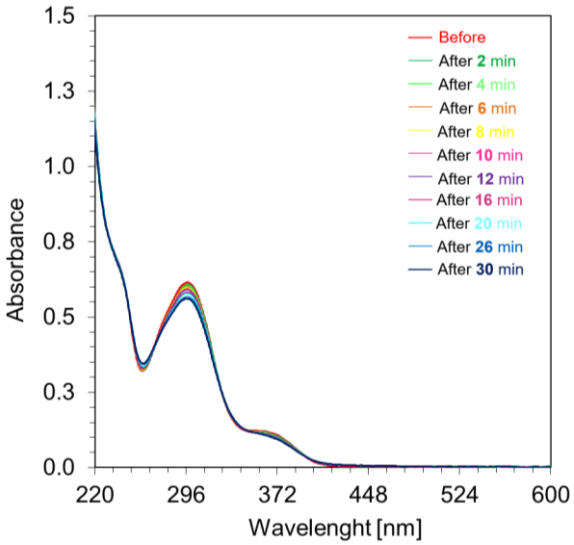


**Figure S75:** Photolysis of BI-PH-O-$CH_3$ in ACN under 365nm (190mW/$cm^2$).

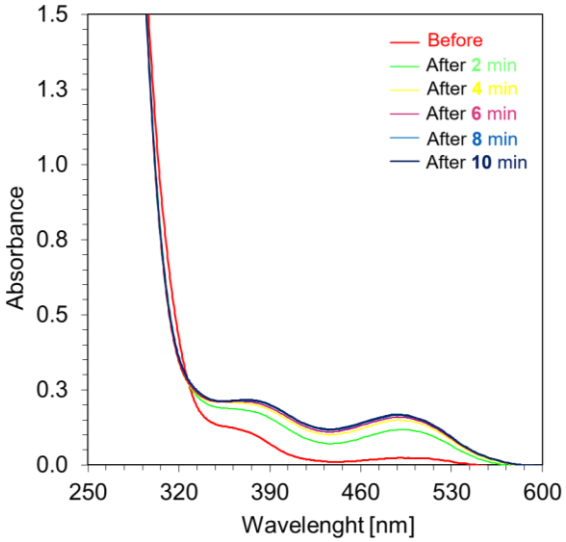


**Figure S76:** Photolysis of BI-PH-O-$CH_3$ + Speedcure 938 (concentration: 1,59·$10^{-3}$ [mol/$dm^3$]) in ACN under 365nm (190mW/$cm^2$).

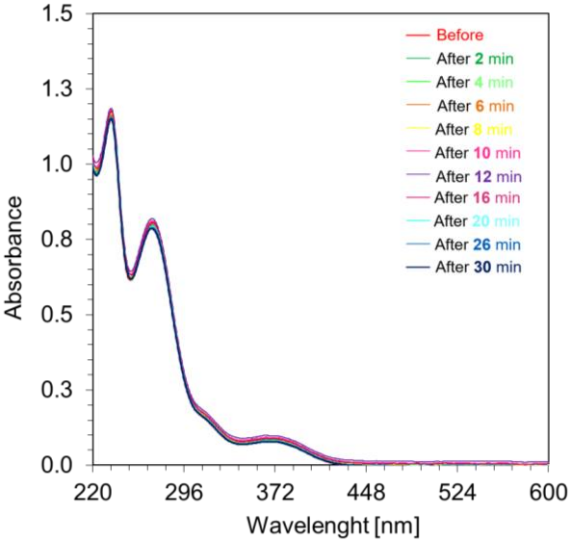


**Figure S77:** Photolysis of BI-PH-CN in ACN under 365nm (190mW/$cm^2$).

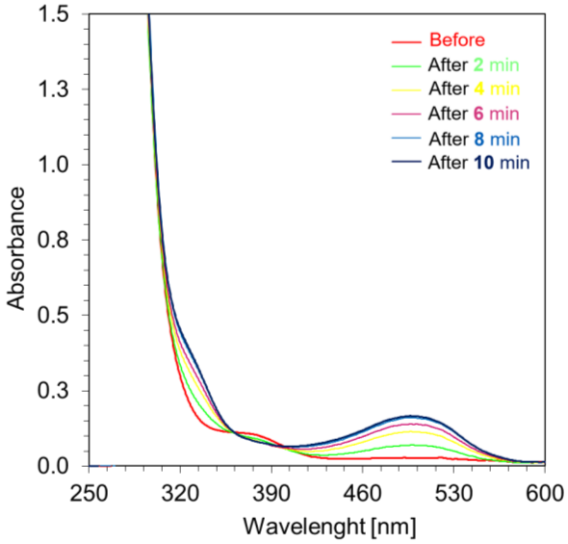


**Figure S78:** Photolysis of BI-PH-CN + Speedcure 938 (concentration: 1,59·$10^{-3}$ [mol/$dm^3$]) in ACN under 365nm (190mW/$cm^2$).

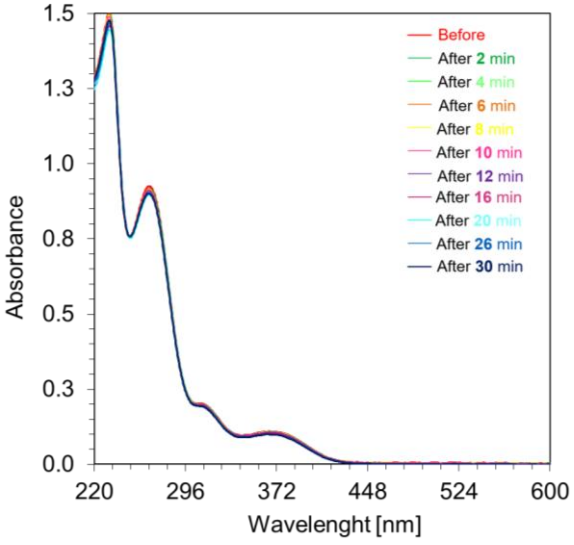


**Figure S79:** Photolysis of BI-PH-$SO_2$-$CH_3$ in ACN under 365nm (190mW/$cm^2$).

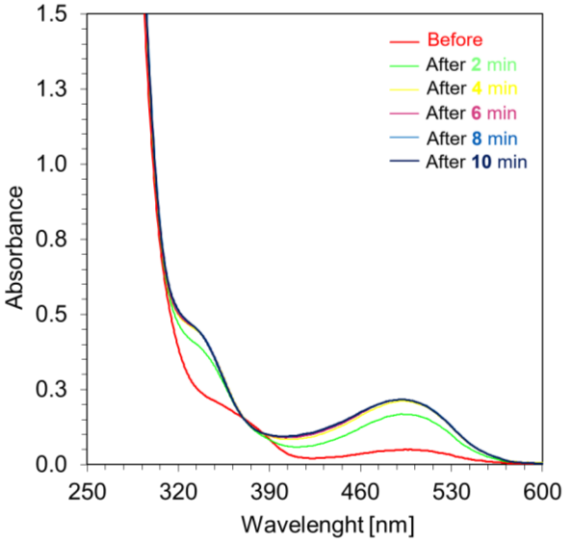


**Figure S80:** Photolysis of BI-PH-$SO_2$-$CH_3$ + Speedcure 938 (concentration: 1,59·$10^{-3}$ [mol/$dm^3$]) in ACN under 365nm (190mW/$cm^2$).

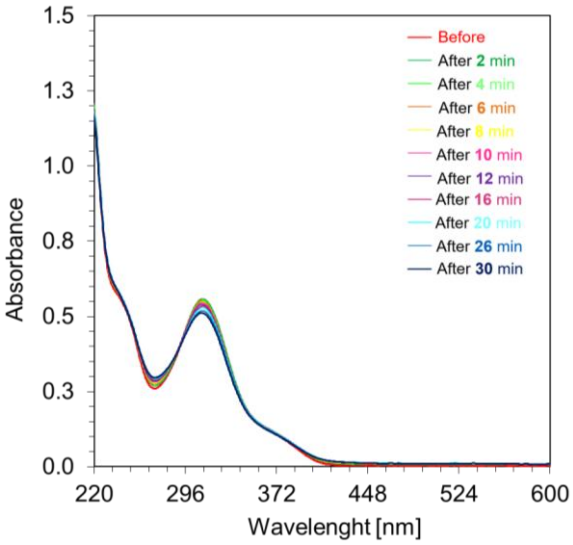


**Figure S81:** Photolysis of BI-PH-S-$CH_3$ in ACN under 365nm (190mW/$cm^2$).

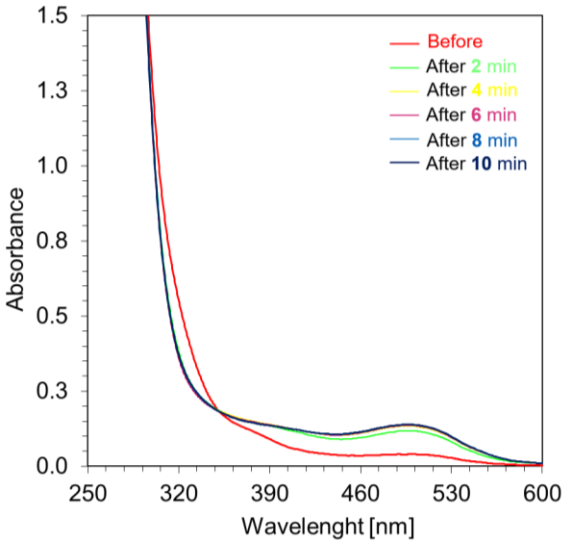


**Figure S82:** Photolysis of BI-PH-S-$CH_3$ + Speedcure 938 (concentration: 1,59·$10^{-3}$ [mol/$dm^3$]) in ACN under 365nm (190mW/$cm^2$).

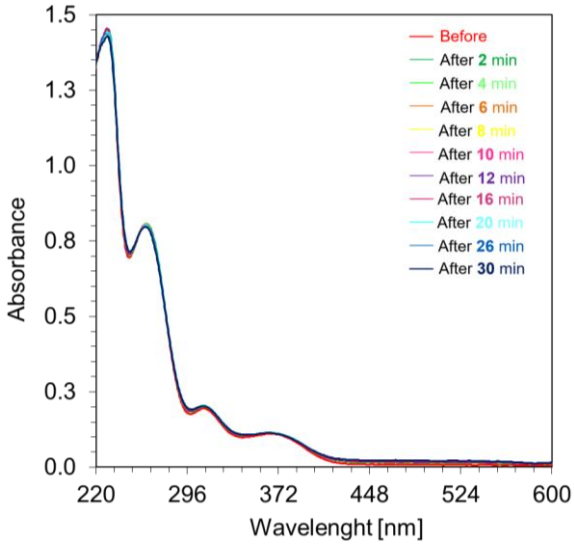


**Figure S83:** Photolysis of BI-PH-$CF_3$ in ACN under 365nm (190mW/$cm^2$).

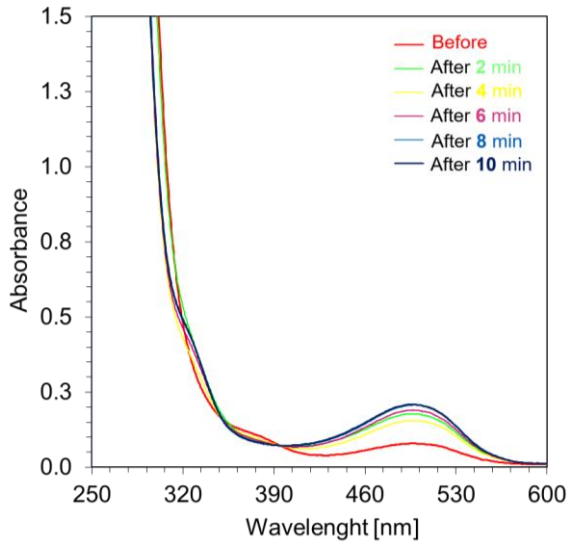


**Figure S84:** Photolysis of BI-PH-$CF_3$ + Speedcure 938 (concentration: 1,59·$10^{-3}$ [mol/$dm^3$]) in ACN under 365nm (190mW/$cm^2$).

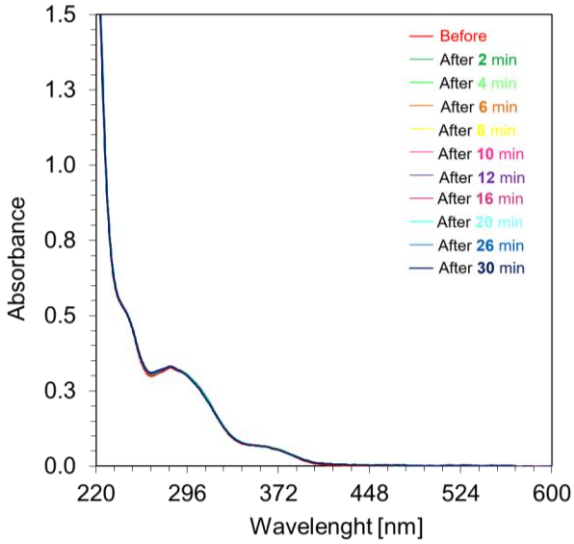


**Figure S85:** Photolysis of BI-1-NPH in ACN under 365nm (190mW/$cm^2$).

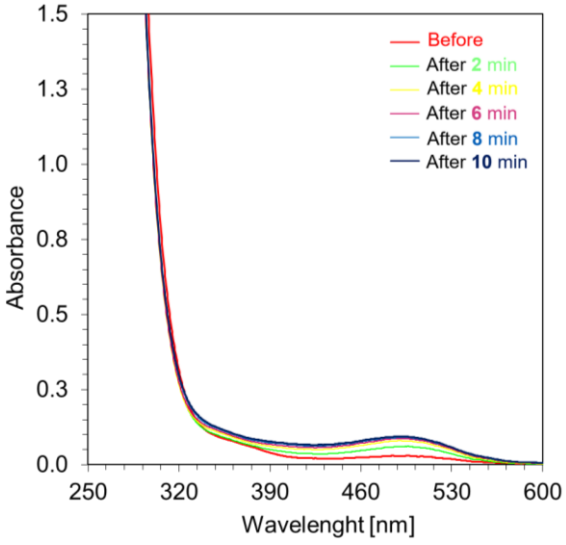


**Figure S86:** Photolysis of BI-1-NPH + Speedcure 938 (concentration: 1,59·$10^{-3}$ [mol/$dm^3$]) in ACN under 365nm (190mW/$cm^2$).

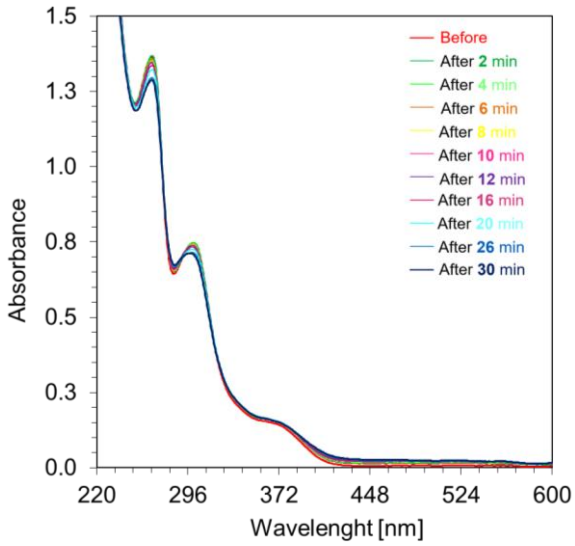


**Figure S87:** Photolysis of BI-2-NPH in ACN under 365nm (190mW/cm$^2$).

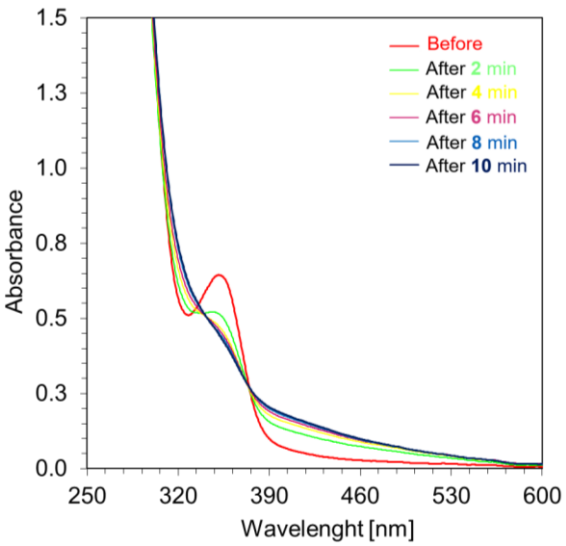


**Figure S88:** Photolysis of BI-2-NPH + Speedcure 938 (concentration: 1,59·10$^{-3}$ [mol/dm$^3$]) in ACN under 365nm (190mW/cm$^2$).

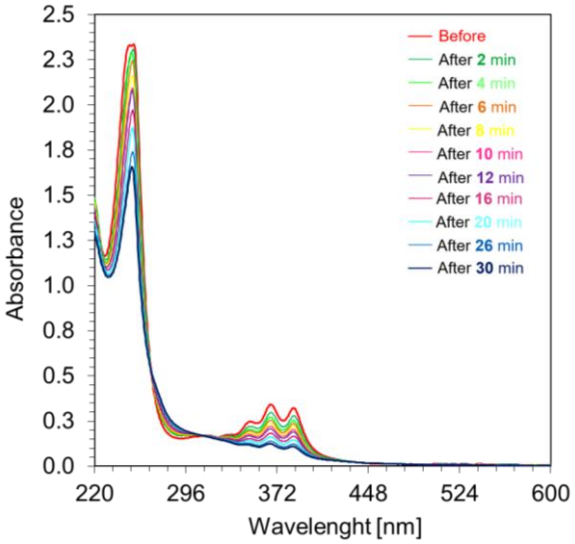


**Figure S89:** Photolysis of BI-1-AN in ACN under 365nm (190mW/cm$^2$).

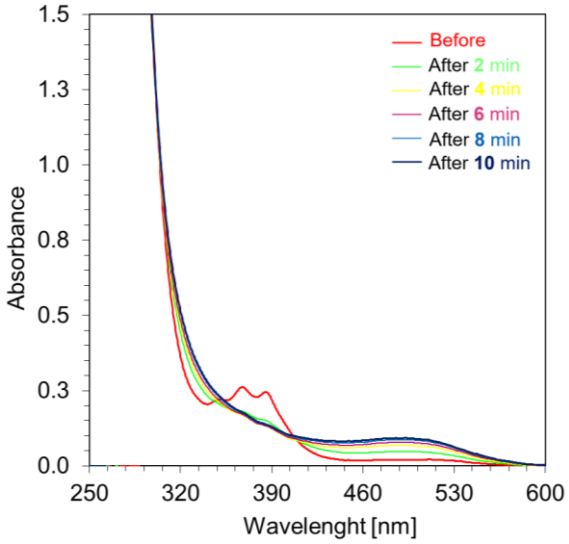


**Figure S90:** Photolysis of BI-1-AN + Speedcure 938 (concentration: 1,59·10$^{-3}$ [mol/dm$^3$]) in ACN under 365nm (190mW/cm$^2$).

## Lifetime of 2-(diethylamino)-4-methyl-6-phenyl-benzene-1,3-dicarbonitrile derivatives in acetonitrile

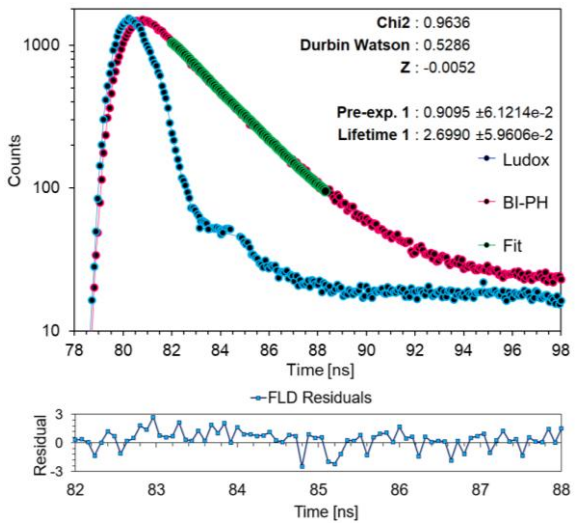


**Figure S91:** Fluorescence lifetime decay curves of BI-PH derivative with excitation pulse at 320 nm in ACN.

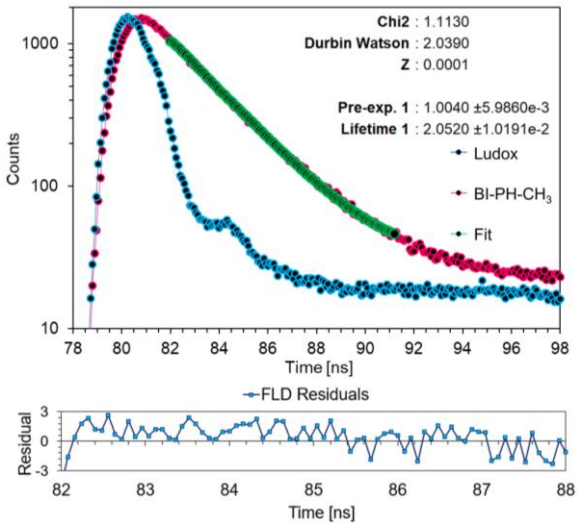


**Figure S92:** Fluorescence lifetime decay curves of BI-PH-$CH_3$ derivative with excitation pulse at 320 nm in ACN.

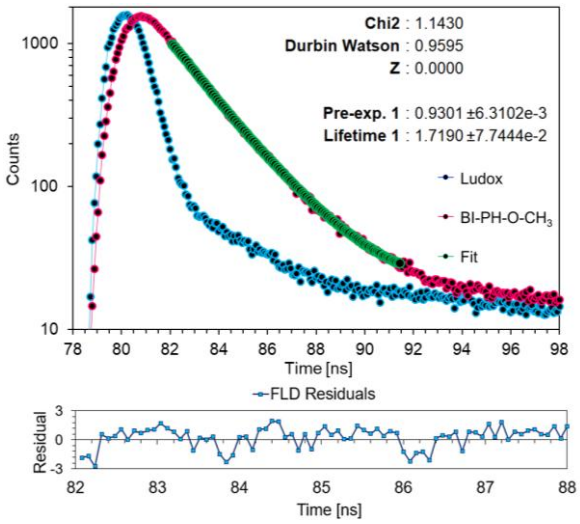


**Figure S93:** Fluorescence lifetime decay curves of BI-PH-O-$CH_3$ derivative with excitation pulse at 320 nm in ACN.

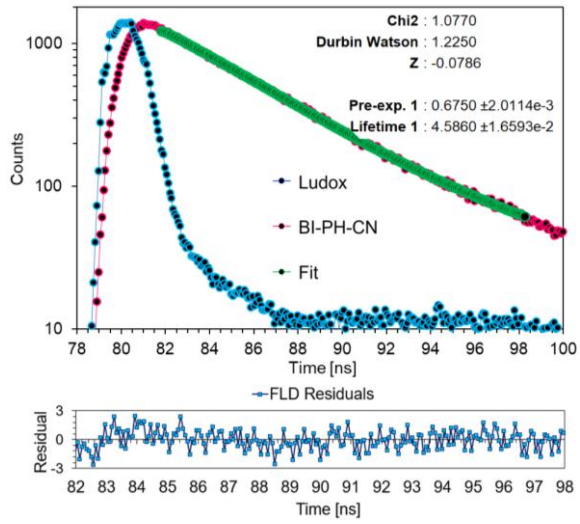


**Figure S94:** Fluorescence lifetime decay curves of BI-PH-CN derivative with excitation pulse at 320 nm in ACN.

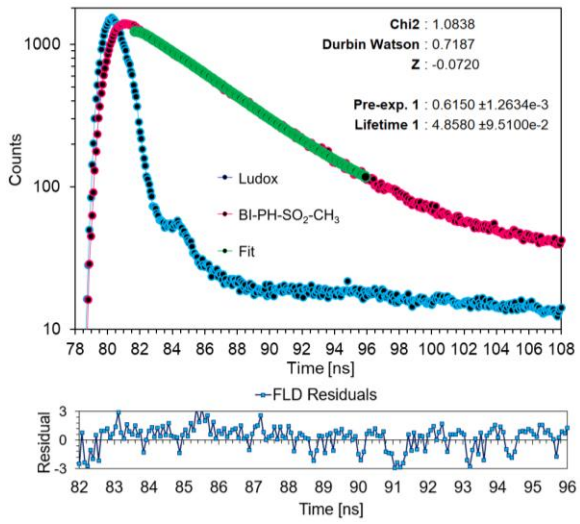


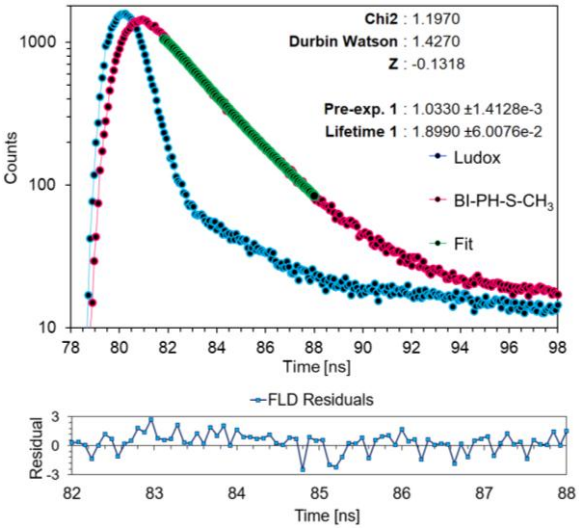

**Figure S95:** Fluorescence lifetime decay curves of BI-PH-$SO_2$-$CH_3$ derivative with excitation pulse at 320 nm in ACN.

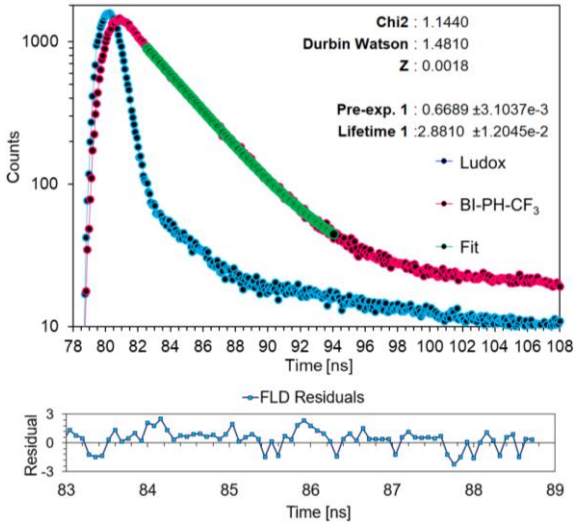


**Figure S96:** Fluorescence lifetime decay curves of BI-PH-S-$CH_3$ derivative with excitation pulse at 320 nm in ACN.

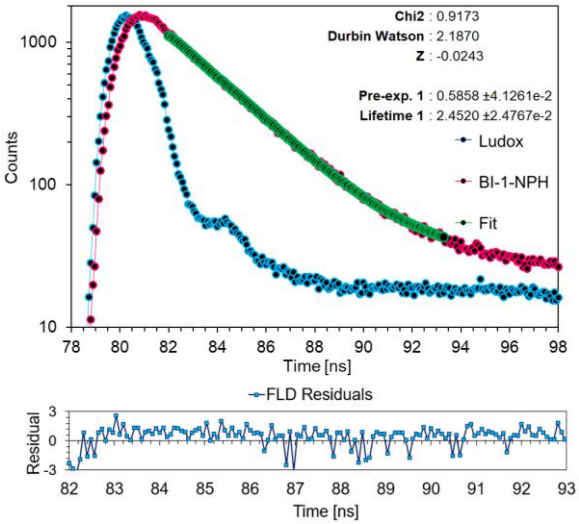


**Figure S97:** Fluorescence lifetime decay curves of BI-PH-$CF_3$ derivative with excitation pulse at 320 nm in ACN.

**Figure S98:** Fluorescence lifetime decay curves of BI-1-NPH derivative with excitation pulse at 320 nm in ACN.

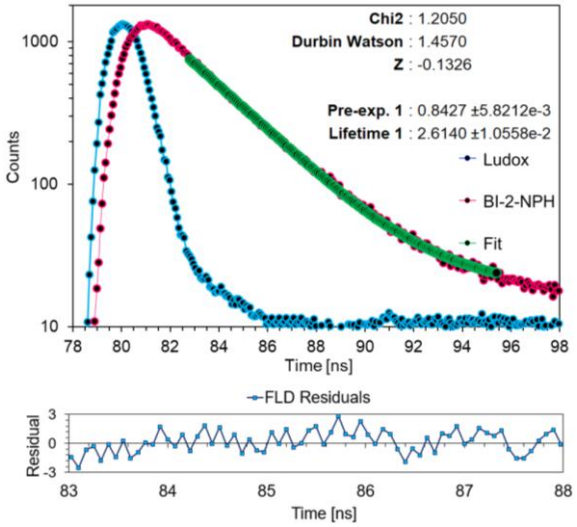


**Figure S99:** Fluorescence lifetime decay curves of BI-2-NPH derivative with excitation pulse at 320 nm in ACN.

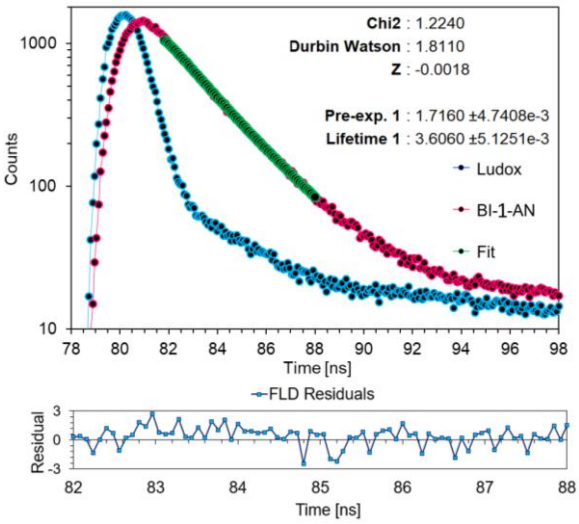


**Figure S100:** Fluorescence lifetime decay curves of BI-1-AN derivative with excitation pulse at 320 nm in ACN.

**Free-radical photopolymerization profile under irradiation at 365 nm (3.77 mW/cm²).**

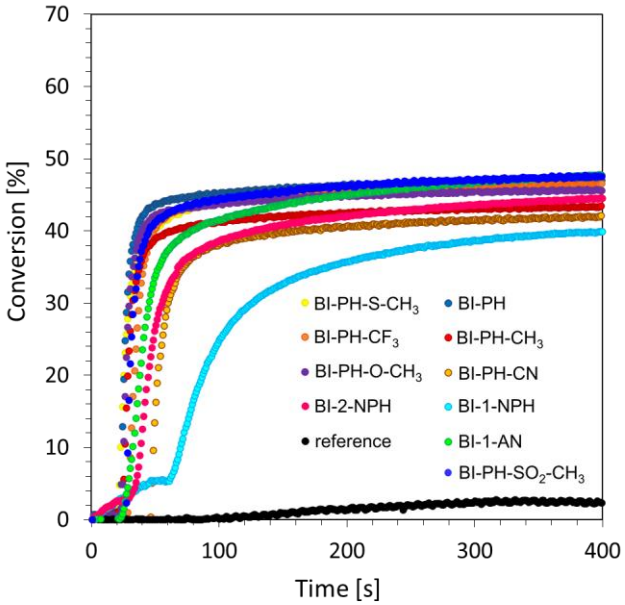


**Figure S101:** Free-radical photopolymerization profiles (double bond conversion vs. irradiation time) initiated by two-component photoinitiating system based on Speedcure 938 (1% wt.) and 2-(diethylamino)-4-methyl-6-phenyl-benzene-1,3-dicarbonitrile derivatives (0.1% wt.) under air and irradiation at 365 nm (3.77 mW/cm$^2$).

**Cationic photopolymerization profile under irradiation at @365 nm (3.77 mW/cm$^2$).**

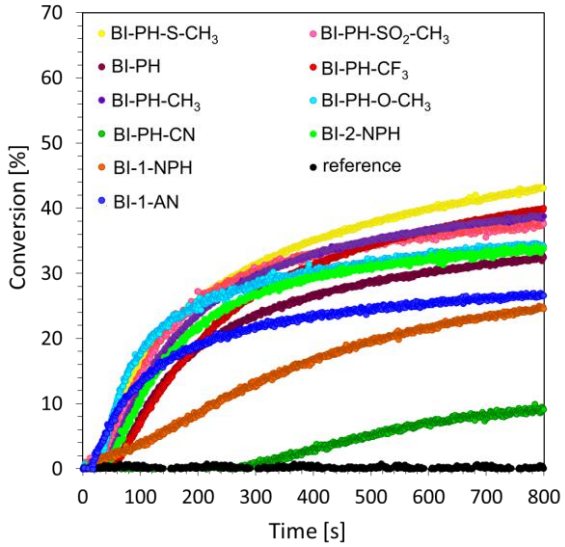


**Figure S102:** Cationic photopolymerization profiles (epoxy function conversion vs. irradiation time) initiated by two-component photoinitiating system based on Speedcure 938 (1% wt.) and 2-(diethylamino)-4-methyl-6-phenyl-benzene-1,3-dicarbonitrile derivatives (0.1% wt.) under irradiation at 365 nm (3.77 mW/cm$^2$).

**Polymerization profiles during profile during the formation of interpenetrating polymer networks under irradiation at @365 nm (3.77 mW/cm²) for monomer TRITHIOL and TRIVNYL**

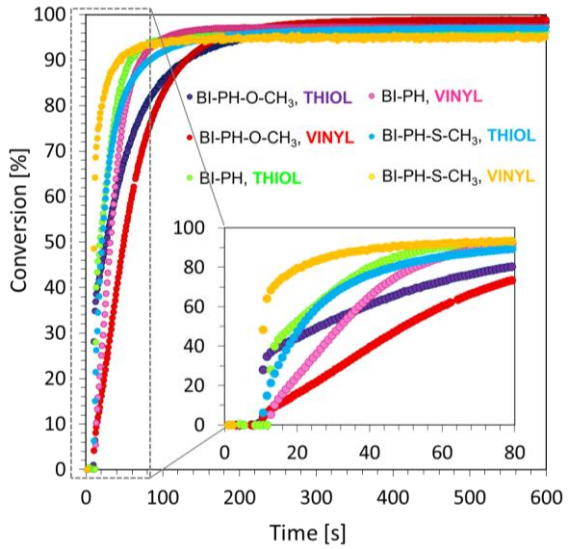


**Figure S103:** Values of conversion of formation IPNs from monomer TRITHIOL and TRIVINYL (0,21:0,79 w/w) in the air at 365 nm (3.77 mW/cm²).

**Polymerization profiles during the formation of interpenetrating polymer networks in various in different measurement conditions for monomer CADE, TMPTA and M100**

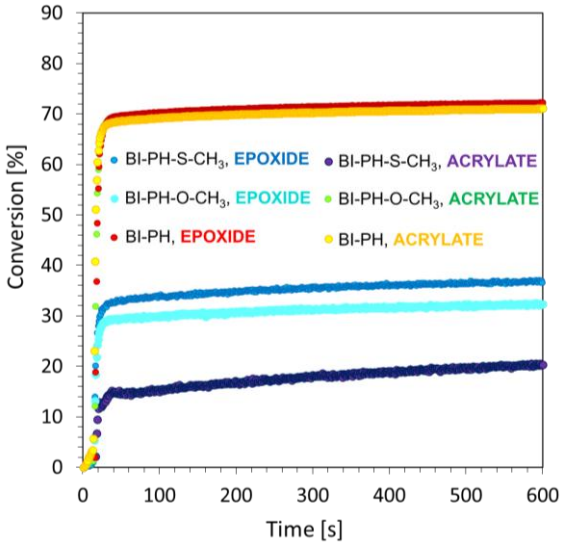


**Figure S104:** Polymerization profiles carried out in laminate, for the system: CADE/TMPTA (1:1 % wt.), + biphenyl derivatives/Iod (0.3/1 %w/w) under irradiation at @ nm (3,77mW/cm²).

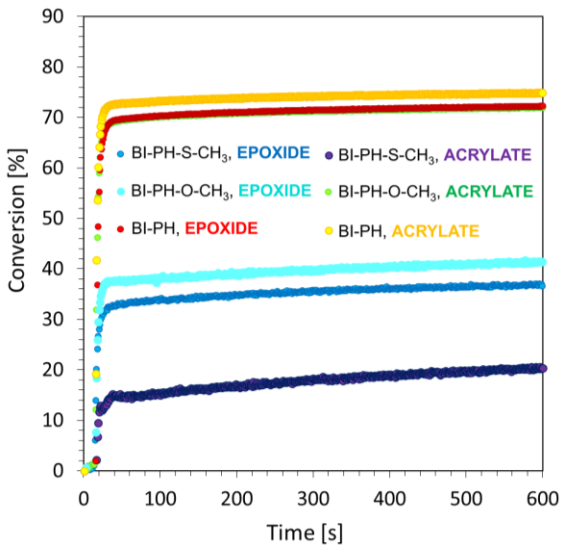


**Figure S105:** Polymerization profiles carried out in laminate, for the system: CADE/TMPTA (1:1 % wt.), + biphenyl derivatives/Iod (0.3/1 %w/w) under irradiation at @405 nm (19.82 mW/cm²).

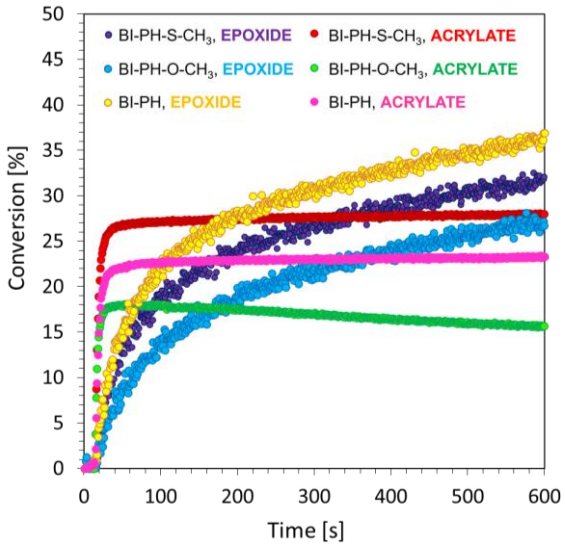


**Figure S106:** Polymerization profiles carried out in the air, for the system: CADE/TMPTA (1:1 % wt.), + biphenyl derivatives/Iod (0.3/1 %w/w) under irradiation at @ nm (3,77mW/cm$^2$).

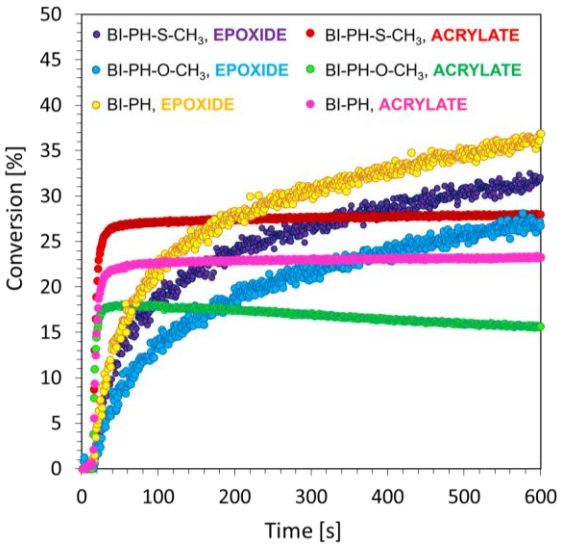


**Figure S107:** Polymerization profiles carried out in the air, for the system: CADE/TMPTA (1:1 % wt.), + biphenyl derivatives/Iod (0.3/1 %w/w) under irradiation at @405 nm (19.82 mW/cm$^2$).

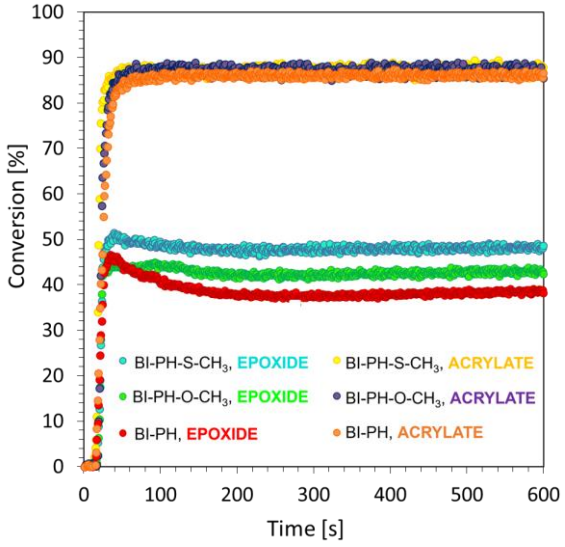


**Figure S108:** Polymerization profiles carried out in thick layer, for the system: CADE/TMPTA (1:1 % wt.), + biphenyl derivatives/Iod (0.3/1 %w/w) under irradiation at @ nm (3,77mW/cm$^2$).

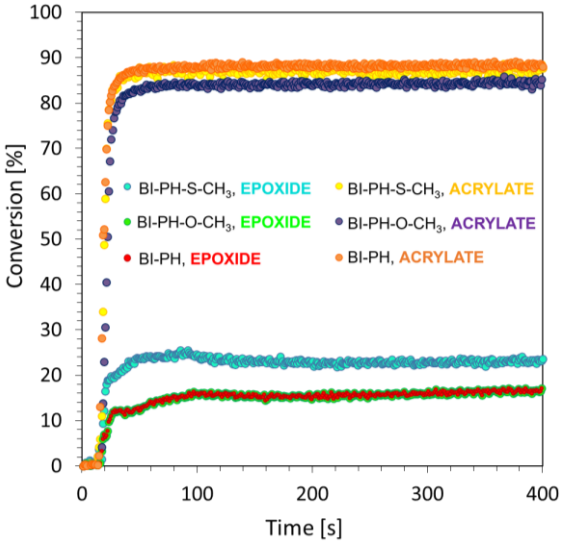


**Figure S109:** Polymerization profiles carried out in thick layer, for the system: CADE/TMPTA (1:1 % wt.), + biphenyl derivatives/Iod (0.3/1 %w/w) under irradiation at @405 nm (19.82 mW/cm$^2$).

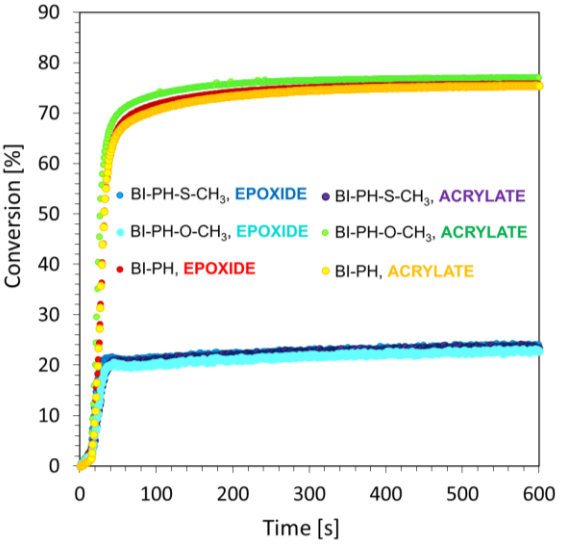


**Figure S110:** Polymerization profiles carried out in laminate,

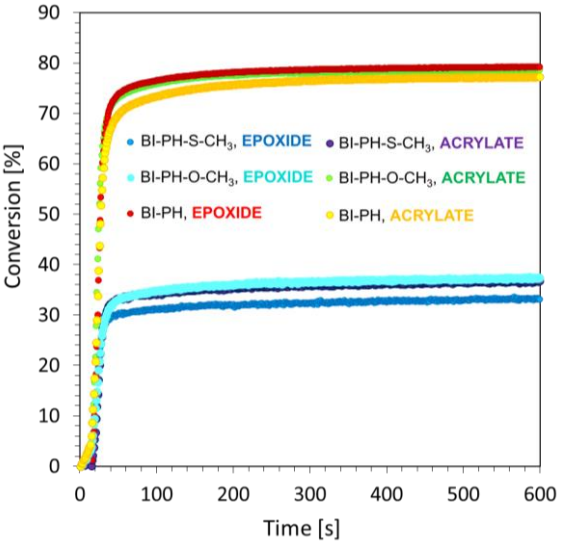


**Figure S111:** Polymerization profiles carried out in laminate,

for the system: CADE/TMPTA/M100 (1:1:1 % wt.),
+ biphenyl derivatives/Iod (0.3/1 %w/w)
under irradiation at @ nm (3,77mW/cm$^2$).

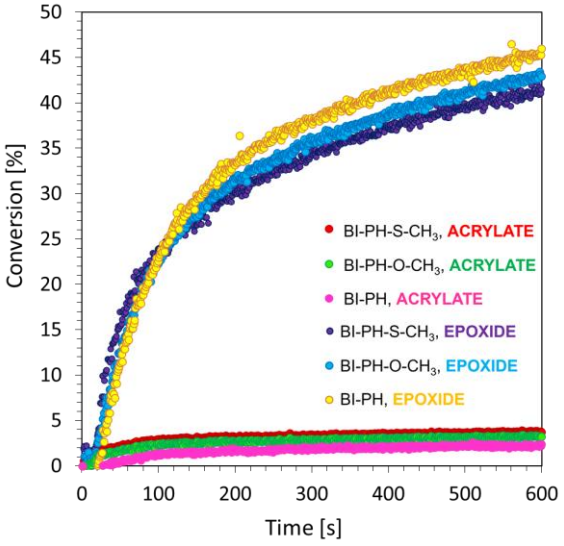


**Figure S112:** Polymerization profiles carried out in the air, for the system: CADE/TMPTA/M100 (1:1:1 % wt.), + biphenyl derivatives/Iod (0.3/1 %w/w) under irradiation at @ nm (3,77mW/cm$^2$).

for the system: CADE/TMPTA/M100 (1:1:1 % wt.),
+ biphenyl derivatives/Iod (0.3/1 %w/w)
under irradiation at @405 nm (19.82 mW/cm$^2$).

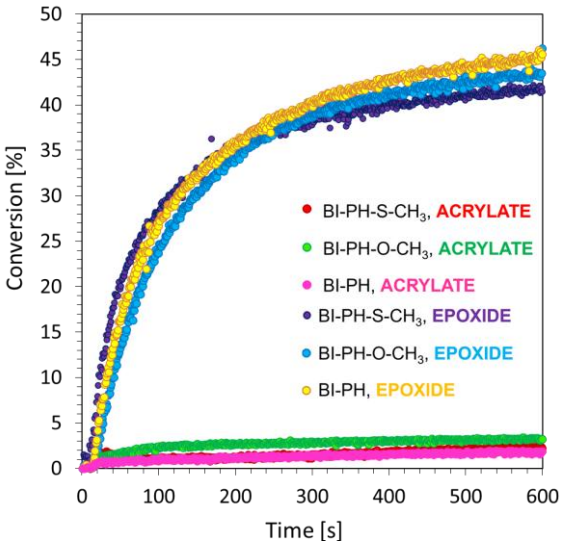


**Figure S113:** Polymerization profiles carried out in the air, for the system: CADE/TMPTA/M100 (1:1:1 % wt.), + biphenyl derivatives/Iod (0.3/1 %w/w) under irradiation at @405 nm (19.82 mW/cm$^2$).

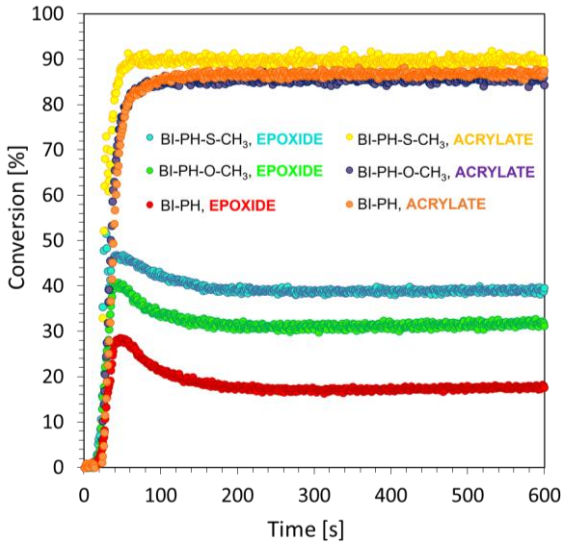


**Figure S114:** Polymerization profiles carried out in thick layer, for the system: CADE/TMPTA/M100 (1:1:1 % wt.), + biphenyl derivatives/Iod (0.3/1 %w/w) under irradiation at @ nm (3,77mW/cm$^2$).

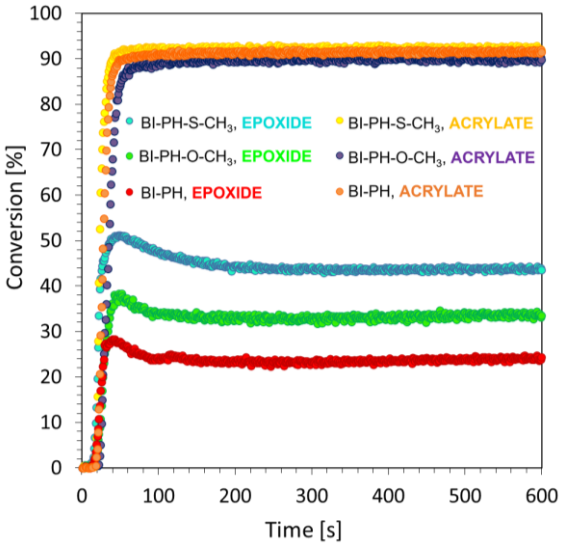


**Figure S115:** Polymerization profiles carried out in thick layer, for the system: CADE/TMPTA/M100 (1:1:1 % wt.), + biphenyl derivatives/Iod (0.3/1 %w/w) under irradiation at @405 nm (19.82 mW/cm$^2$).

## Transmittance spectrum of thin layer of resin with different content od MWCNTs

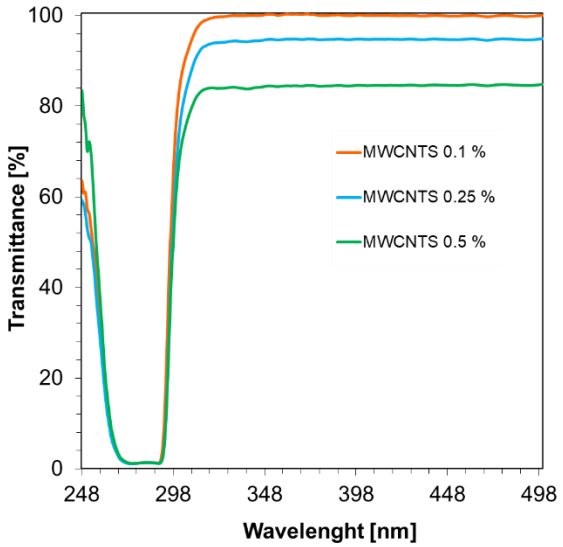


**Figure S116:**. Transmittance spectrum of thin layer of resin with different content od MWCNTs (0.1; 0.25; 0.5 wt. %), without photoinitiating system. The experiment was performed using UV-VIS Spectrophotometer UV-2600i (from Shimadzu).

## Photo-differential scanning calorimetry

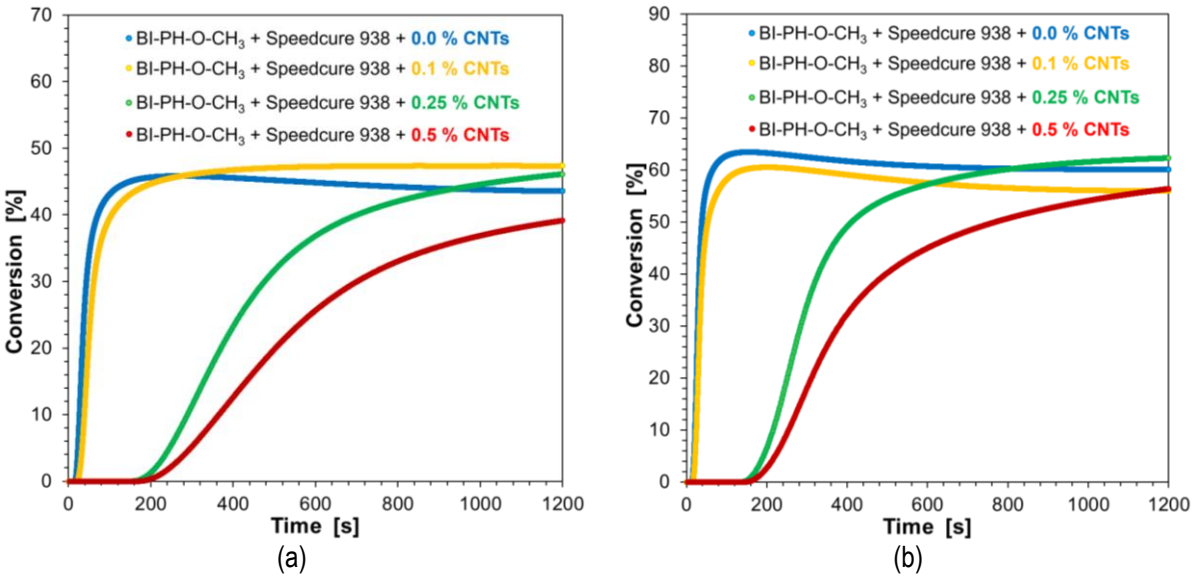


**Figure S117:**. Free-radical photopolymerization profiles for photocurable composites: BI-PH-O-CH3 (0,1% wt.), polymerized at 365 nm (BisGMA) / (TEGDMA) (50 %/50 % w/w) with Speedcure 938 (1 % wt.) a) at 25°C, b) at 70°C.

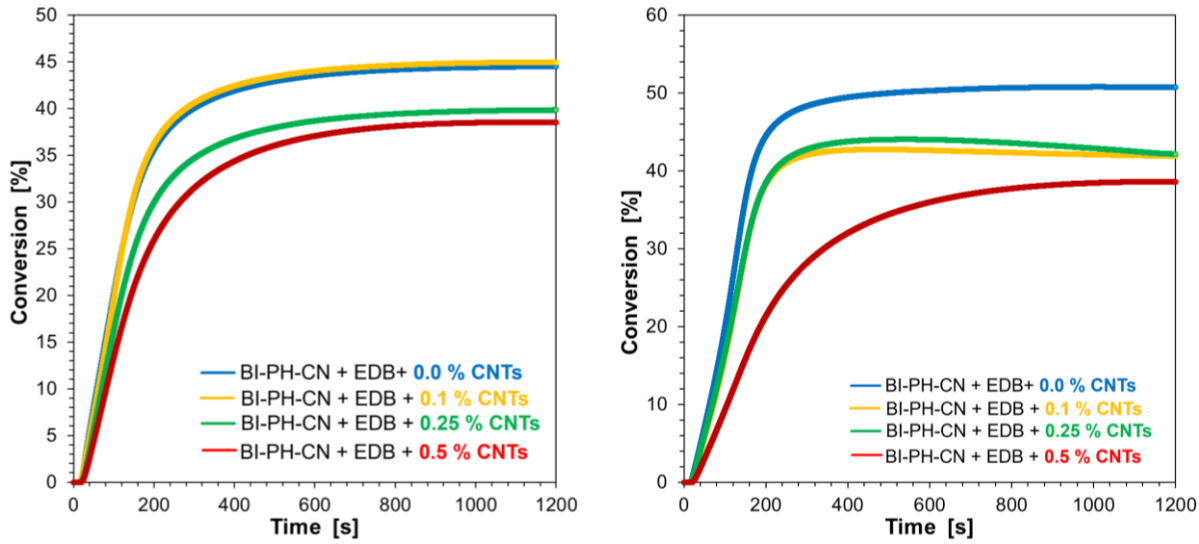


**Figure S118:** Free-radical photopolymerization profiles for photocurable composites: BI-PH-CN (0.1 %wt.), (BisGMA) / (TEGDMA) (50 %/50 % w/w) with EDB (1.5 % wt.) a) at 25°C, b) at 70°C.